

1 **The River Orontes in Syria and Turkey: downstream variation of fluvial archives in different**  
2 **crustal blocks**

3  
4 David R. Bridgland <sup>a,\*</sup>, Rob Westaway <sup>b,c</sup>, Mohammad Abou Romieh <sup>d</sup>, Ian Candy <sup>e</sup>, Mohamad  
5 Daoud <sup>d</sup>, Tuncer Demir <sup>f</sup>, Nikolaos Galiatsatos <sup>a</sup>, Danielle C. Schreve <sup>e</sup>, Ali Seyrek <sup>g</sup>, Andrew D.  
6 Shaw <sup>h</sup>, Tom White <sup>i</sup>, John Whittaker <sup>j</sup>

7  
8 <sup>a</sup> *Department of Geography, Durham University, South Road, Durham DH1 3LE, UK*

9 <sup>b</sup> *Faculty of Mathematics, Computing and Technology, The Open University, Abbots Hill, Gateshead*  
10 *NE8 3DF, UK*

11 <sup>c</sup> *Newcastle Institute for Research on Sustainability (NIReS), Newcastle University, Newcastle-*  
12 *upon-Tyne NE1 7RU, UK*

13 <sup>d</sup> *National Earthquake Center, Rasheed Karamah Street, Al-Adawi, Damascus, Syria*

14 <sup>e</sup> *Department of Geography, Royal Holloway, University of London, Egham, Surrey TW20 0EX, UK*

15 <sup>f</sup> *Department of Geography, Harran University, 63300 Şanlıurfa, Turkey*

16 <sup>g</sup> *Department of Soil Science, Harran University, 63300 Şanlıurfa, Turkey*

17 <sup>h</sup> *Department of Archaeology, University of Southampton, Highfield, Southampton SO17 1BJ, UK*

18 <sup>i</sup> *Department of Zoology, University of Cambridge, Cambridge CB2 3EJ, UK*

19 <sup>j</sup> *Department of Palaeontology, Natural History Museum, Cromwell Road, London SW7 5BD, UK*

20  
21 *Corresponding author.*

22 *Email address: d.r.bridgland@durham.ac.uk*

23  
24 **ABSTRACT**

25 The geomorphology and Quaternary history of the River Orontes in western Syria and south-central  
26 Turkey have been studied using a combination of methods: field survey, differential GPS, satellite  
27 imagery, analysis of sediments to determine provenance, flow direction and fluvial environment,  
28 incorporation of evidence from fossils for both palaeoenvironments and biostratigraphy, uranium-  
29 series dating of calcrete cement, reconciliation of Palaeolithic archaeological contents, and uplift  
30 modelling based on terrace height distribution. The results underline the contrasting nature of  
31 different reaches of the Orontes, in part reflecting different crustal blocks, with different histories of  
32 landscape evolution. Upstream from Homs the Orontes has a system of calcreted terraces that  
33 extends to ~200 m above the river. New U-series dating provides an age constraint within the lower  
34 part of the sequence that suggests underestimation of terrace ages in previous reviews. This upper  
35 valley is separated from another terraced reach, in the Middle Orontes, by a gorge cut through the

36 Late Miocene–Early Pliocene Homs Basalt. The Middle Orontes terraces have long been  
37 recognized as a source of mammalian fossils and Palaeolithic artefacts, particularly from Latamneh,  
38 near the downstream end of the reach. This terraced section of the valley ends at a fault scarp,  
39 marking the edge of the subsiding Ghab Basin (a segment of the Dead Sea Fault Zone), which has  
40 been filled to a depth of ~1 km by dominantly lacustrine sediments of Pliocene–Quaternary age.  
41 Review of the fauna from Latamneh suggests that its age is 1.2–0.9 Ma, significantly older than  
42 previously supposed, and commensurate with less uplift in this reach than both the Upper and  
43 Lower Orontes. Two localities near the downstream end of the Ghab have provided molluscan and  
44 ostracod assemblages that record somewhat saline environments, perhaps caused by desiccation  
45 within the former lacustrine basin, although they include fluvial elements. The Ghab is separated  
46 from another subsiding and formerly lacustrine depocentre, the Amik Basin of Hatay Province,  
47 Turkey, by a second gorge, implicit of uplift, this time cut through Palaeogene limestone. The NE–  
48 SW oriented lowermost reach of the Orontes is again terraced, with a third and most dramatic gorge  
49 through the southern end of the Amanos Mountains, which are known to have experienced rapid  
50 uplift, probably again enhanced by movement on an active fault. Indeed, a conclusion of the  
51 research, in which these various reaches are compared, is that the crust in the Hatay region is  
52 significantly more dynamic than that further upstream, where uplift has been less rapid and less  
53 continuous.

54 Keywords:

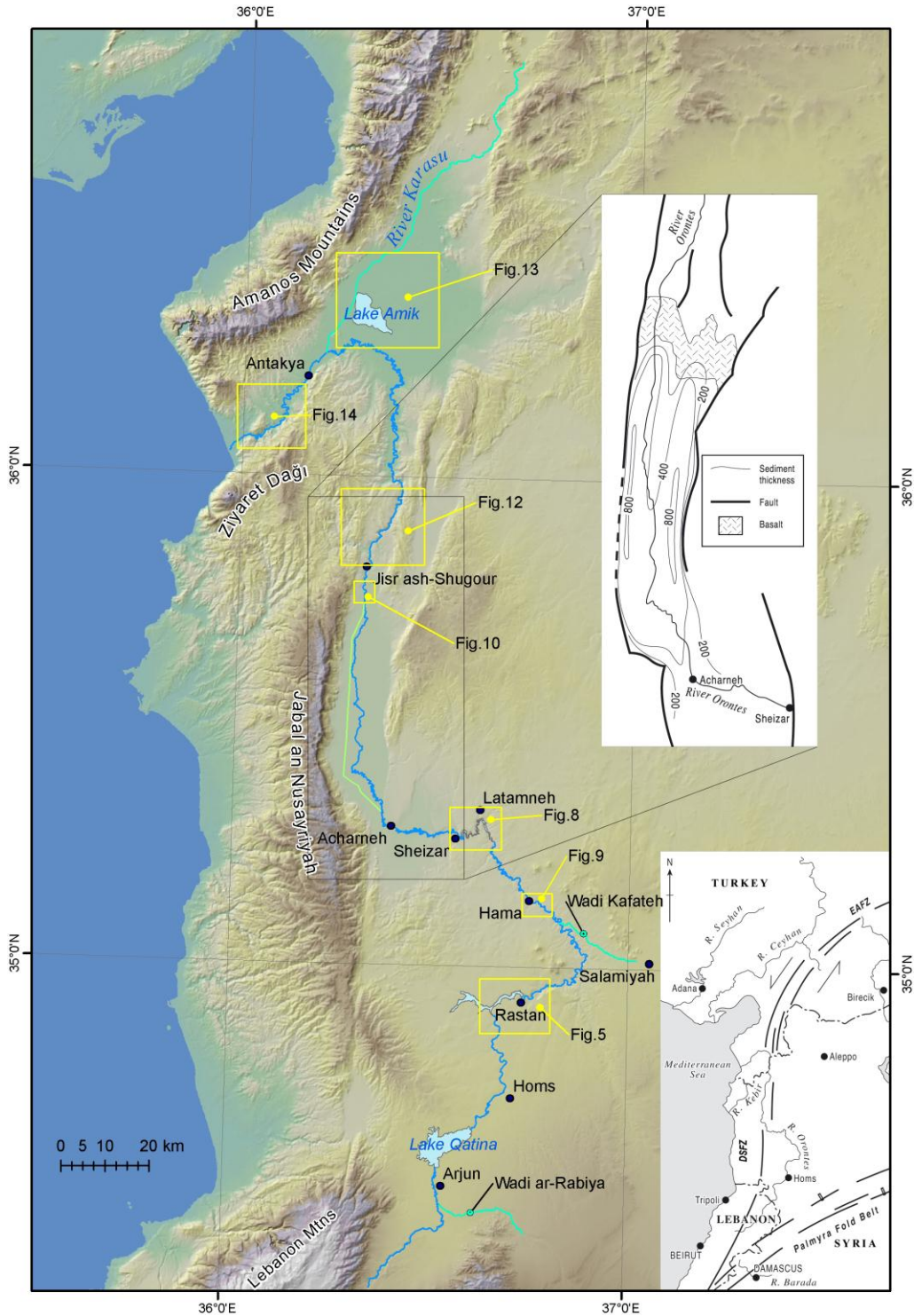
55 River Orontes; river terraces; fluvial deposits; uplift; subsidence

56

## 57 **1. Introduction**

58 The Orontes (‘Asi’ in Arabic) is the principal river draining to the Levant coastline of the  
59 Mediterranean Sea. From its source in the Bekaa Valley of Lebanon, on the flank of the Lebanon  
60 mountain range, it flows northwards across western Syria through the cities of Homs and Hama and  
61 into Hatay Province, southern Turkey, before turning sharply south-westward to reach the sea  
62 ~30 km downstream of Antakya (Fig. 1). In north-west Syria the Orontes forms the axial drainage  
63 of the Ghab Basin, a linear valley marking the Dead Sea Fault Zone (DSFZ), the boundary between  
64 the African plate (to the west) and the Arabian plate (to the east), along which left-lateral relative  
65 plate motion is accommodated (Fig. 1). Upstream of the Ghab Basin, the terrace sequence of the  
66 Middle Orontes has been well documented, largely on account of attention from archaeologists  
67 interested in its Palaeolithic contents (e.g. Burkhalter, 1933; Modderman, 1964; Van Liere, 1966;

68 Clark, 1966a, b, c, 1967, 1968, Besançon et al., 1978a, b; Besançon and Sanlaville, 1993a;  
 69 Dodonov et al., 1993; Bartl and al-Maqqdissi, 2005). Indeed, the work described here stemmed  
 70 initially from an archaeological survey of the Homs region (Philip et al., 2005), which included



71  
 72 **Fig. 1.** Course of the Orontes in relation to topography (main image, a DEM derived from SRTM) and structural setting (lower inset).  
 73 Locations are shown of places described in the paper and of other figures. Abbreviations: DSFZ = Dead Sea Fault Zone; EAFZ =  
 74 East Anatolian Fault Zone. The upper inset shows the fault control and sediment thickness of the Ghab Basin.

75 ~700 km<sup>2</sup> of the upper catchment of the Orontes. An extensive sequence of river terraces,  
 76 previously unrecognized as such, was recorded in the upper Orontes valley as a result of this

77 initiative (Bridgland et al., 2003; Bridgland and Westaway, 2008a). In seeking to obtain a full  
78 understanding of the context for this newly discovered long-timescale fluvial record, research on the  
79 Orontes was extended downstream and has now been undertaken along the length of the valley  
80 between Homs and the Mediterranean, revealing marked contrasts between different reaches.  
81 Separating the upper and middle catchments, both of which have terraces, is a gorge, named after  
82 the town of Rastan, ~25 km north of Homs. Two further gorges occur: one between the Ghab Basin  
83 and the border with Hatay Province and the other downstream of Antakya. They are separated by  
84 another former lacustrine basin (Fig. 1), occupied until the mid 20th Century by Lake Amik.

85 This paper relates how multi-disciplinary research has allowed the complex and contrasting records  
86 from different reaches of this unusual river course to be reconstructed and reconciled one with  
87 another. Methods have included field survey, recording and analyses of fluvial sediments, remote  
88 surveying of fluvial landforms (both depositional and erosional) and the use of Geographical  
89 Information Systems (GIS) techniques to obtain height data (of considerable value in areas remote  
90 from known-height markers such as bench marks). Also valuable has been the study of the fossil  
91 and artefact contents of the Orontes deposits, which have provided information on palaeo-  
92 environments and possible ages. In addition, the incision recorded by river terraces, which is  
93 interpreted as a response to uplift, can be modelled mathematically against time, using computer  
94 programs designed for the purpose (Westaway, 2002, 2004a; Westaway et al., 2002). These take  
95 account of forcing mechanisms that affect the rate of uplift, which are considered to be driven by  
96 climatic fluctuation and linked to surface processes, with the aim of providing an age framework for  
97 the interpretation of terrace sequences (Bridgland and Westaway, 2008a, b; Westaway et al.,  
98 2009a). This approach has been applied previously to the upper Orontes terrace sequence  
99 (Bridgland et al., 2003; Bridgland and Westaway, 2008a; see below).

100 The aim of the paper is to establish age-related stratigraphical frameworks for those reaches with  
101 accessible sedimentary evidence, in the form of river terraces, by pooling the available evidence and  
102 applying the most appropriate of the above-mentioned techniques. This will allow correlation and  
103 comparison between these reaches and also demonstrate the contrast with reaches in which terraces  
104 have not been developed. The importance of these findings is that they can be related to different  
105 histories of valley evolution in different reaches, corresponding with separate crustal blocks, for  
106 which the causes can be discussed in terms of crustal deformation.

## 107 **2. Survey methods**

108 Orontes river terraces have been mapped previously between Rastan and the Ghab Basin, based on  
109 surveys by geologists and archaeologists in the 1970s and '80s (Besançon et al., 1978a, b; Besançon  
110 and Sanlaville, 1993a; Dodonov et al., 1993). The resultant maps, although detailed, have been  
111 found to simplify the complexity of the terrace sequence and to be heavily dependent on  
112 geomorphology, with little attention paid to underlying fluvial sediment bodies. Nonetheless, these  
113 pre-existing maps represent an excellent resource and, with 'ground-truthing', are superior to  
114 anything yet produced in most other reaches, where the more recent surveys conducted by the  
115 authors are, by comparison, rudimentary. The only other reach of the Orontes that has hitherto been  
116 documented in comparable detail is that between Antakya and the coast, described by Erol (1963).  
117 Given the constraints of research visits of limited extent, the recent surveys have relied on a  
118 combination of different GIS resources, with field surveys designed to determine the terrace  
119 sequence at key points along the course. The locations of these were often determined by  
120 accessibility and permissions, although published sources of Palaeolithic and palaeontological  
121 evidence were targeted for investigation and re-survey, and searches for new data of these types  
122 were undertaken wherever possible.

123 New and supplementary mapping, including topographic information, has made use of differential  
124 global positioning system (dGPS) equipment, specifically Leica System 300, operated in static  
125 survey mode, with reference to temporary base stations on high points and to known heights such as  
126 bench marks. Optimal results were obtained when the roving station occupied each survey point for  
127 at least 100 two-second recording epochs and in cases where such points were not more than 50 km  
128 from the base station. Under favourable conditions, however, the technique has been shown to  
129 work satisfactorily with the base station and roving stations up to 100 km apart (cf. Demir et al.,  
130 2009, this issue). At certain locations, with limited sky visibility, it was necessary to survey to a  
131 point in the open and calculate the distance and height difference, the latter making use of an Abney  
132 level. In the earlier surveys, generally those in the Upper Orontes, the dGPS data were processed  
133 using Leica SKI v2.3 software. Later survey data have been processed using Leica GeoOffice  
134 (version 4.1, 5.0 or 5.1), which incorporates an improved algorithm for eliminating phase  
135 ambiguities in its differential GPS solutions (in part because it uses a different approach for treating  
136 propagation delays of GPS signals through the ionosphere) and generally provides better data  
137 resolution. Where original dGPS raw output had been retained it proved possible to reprocess older  
138 data with this improved software but, unfortunately, since the provision of improved software had  
139 not been foreseen, much of the Upper Orontes survey output had been retained only in processed  
140 form.

141 GIS resources have included satellite imagery, with emphasis on CORONA high-resolution  
142 photographic images from 1960–1972, before the large-scale expansion of agriculture (Galiatsatos  
143 et al., 2008), and shuttle radar topographic mission (SRTM) altimetry. Since the 1995  
144 declassification of CORONA (KH-4), it has been thoroughly studied and used in many applications,  
145 mostly related to change detection and photo-interpretation (e.g. Galiatsatos, 2004, 2009; Sohn et  
146 al., 2004; Dashora et al., 2007). The archaeological community has shown a keen interest in  
147 CORONA, particularly in areas where it is difficult to obtain detailed historical photography, such  
148 as the Near East. For the Homs Survey area a digital elevation model (DEM) is now available,  
149 obtained from CORONA and ground-truthed by dGPS. The research reported here has also used  
150 satellite imagery from the Fragile Crescent Project, a large-scale archaeological investigation of the  
151 Middle East (Galiatsatos et al., 2009). In addition to CORONA, the project took advantage of a  
152 GAMBIT image that was acquired on 25 April 1966 in the area of Hama. GAMBIT (or KH-7) was,  
153 like CORONA, a spy satellite program; it flew 38 missions from July 1963 to June 1967 and was  
154 declassified in 2002. It has a spatial resolution of 0.6–1.2 m but, as the relevant documentation  
155 remains classified, little is known about the camera system.

156 Of four versions of SRTM data, Version 1 is the ‘raw’ data, Version 2, used in the present study, is  
157 the result of editing for water bodies and the removal of spikes and wells, whereas Versions 3 and 4  
158 were created and distributed by the CGIAR Consortium for Spatial Information and include  
159 improvements in the filling of voids. The SRTM data used (cf. JPL, 1998a, b, 2005) have a  
160 resolution of 3 arc seconds of latitude, or roughly 90 m, with a global vertical accuracy of better  
161 than 10 m, and horizontal accuracy of ~10 m, depending on the relief of the ground (Rodriguez et  
162 al., 2006). However, various applications from Hungary (Kay et al., 2005), Portugal (Gonçalves  
163 and Fernandes, 2005) and Turkey (Jacobsen, 2005; Westaway et al., 2006, 2009b; Demir et al., this  
164 issue) have demonstrated a vertical accuracy of better than 5 m in a variety of terrain. Data of this  
165 type provide a particularly valuable source of height information for parts of the world where large-  
166 scale topographic maps are not readily available; they can be rendered as DEMs in a range of  
167 formats using standard GIS techniques. Throughout this study, satellite imagery and imagery  
168 generated from SRTM data are displayed using Universal Transverse Mercator (UTM) co-ordinates  
169 expressed using the WGS-84 datum; the same co-ordinate system is therefore used for reporting co-  
170 ordinates of field sites

## 171 **2.1 Supplementary geological techniques**

172 A technique of assistance in terrace surveys is clast-lithological analysis of gravels. This has been  
173 particularly valuable for identifying Orontes deposits and distinguishing them from the products of

174 local (tributary) rivers. Clast analysis of cemented gravels, which are common in certain reaches,  
175 was, of necessity, conducted in the field. A cardboard sieve plate was used to estimate clast size in  
176 order to count only pebbles between the desired sizes of 16 and 32 mm (a recommended standard  
177 size range for such analyses: Bridgland, 1986). This works well enough where gravel components,  
178 such as the limestones and flints/cherts that characterize the Orontes in Syria (Table 1), are readily  
179 distinguished in outcrop, so analyses can be carried out with the aid of a hand lens, a small knife to  
180 determine hardness, 10% HCl for confirmation of calcareous lithologies and a suitable pen to mark  
181 clasts as they are counted. In reaches where the Orontes gravels were less consolidated it was  
182 possible to collect gravel samples and identify loose clasts, although the difficulty and expense of  
183 transporting heavy samples meant that analyses were still conducted during fieldwork; with bagged  
184 samples this could take place during evenings or even during journeys between locations,  
185 optimizing field time for mapping and making records of sections. Downstream of Hama the  
186 Orontes gravels become completely dominated by flint (Table 1), there being a rich source of brown  
187 flint in the Upper Cretaceous chalk and chalky limestone, through which the river has incised (Clark  
188 1967), although flint has also been reported in Palaeogene limestones in the region (Ponikarov,  
189 1986). This flint has provided the raw material for the Palaeolithic industries that are well  
190 represented in the gravels of this reach, and which first drew the attention of researchers to the  
191 Orontes system (e.g., Clark, 1966a, b, 1967, Muhesen, 1985, Copeland and Hours, 1993, Shaw,  
192 2008, in press). The relative monotony of the Middle Orontes gravels, however, means that their  
193 analysis is of less value here. Further downstream, in Hatay, the gravels consist largely of  
194 crystalline rocks from the local area, including the Hatay ophiolite (latest Cretaceous),  
195 supplemented by further travelled material from the Amanos Mountains to the north of Antakya,  
196 derived by way of the River Karasu, a right-bank Orontes tributary (Fig. 1; Table 1).

197

### 198 **3. Upper Orontes: Lebanon border to the Rastan Gorge**

199 The open, low-relief landscape of the Upper Orontes (Fig. 2A), upstream of the Rastan Gorge, is  
200 floored by Neogene lacustrine marl of inferred 'Pontian' (latest Miocene) age (Dubertret and  
201 Vautrin, 1938). This marl is interbedded with the Late Miocene–Early Pliocene Homs basalt, for  
202 which recent re-dating using the Ar–Ar technique indicates an age range of ~6–4 Ma (Searle et al.,  
203 2010; Westaway, 2011), superseding earlier whole-rock K–Ar dating that gave generally older (~8–  
204 5 Ma) numerical ages (Mouty et al., 1992; Sharkov et al., 1994; Butler and Spencer, 1999).  
205 Boreholes east of Homs confirm that marl occurs both above and below the Homs Basalt  
206 (Ponikarov et al., 1963a; Fig. 3), suggesting that lacustrine conditions (possibly caused by the

207 damming of proto-Orontes drainage by the earliest basalt eruptions) persisted into the Pliocene. It  
 208 is also evident, from its interbedding with the marl and from pillow lava formation, seen at a  
 209 number of localities to the north of Homs, that the Homs Basalt erupted into the ‘Pontian’ lake.

210 **Table 1.** Gravel clast lithology counts from deposits attributed to the River Orontes and related systems (in approximate downstream sequence)

Reach	Site	Coordinates	Chert & flint	Limestone	Voids	Quartzite	Basalt	Coarse basaltic	Ophiolite	Others	Total count
Upper Orontes	Al Hauz <sup>1</sup>	BU 73478 28799	53.5	36.0	10.5						275
	Arjun Quarry <sup>2</sup>	BU 74580 25832	33.6	66.4							256
	Al Hussainiyeh	BU 90236 27562	37.9	62.1							253
	Dmaynah <sup>1</sup>	BU 87074 28915	65.9	33.7	0.4						258
	Um al-Sakhr <sup>1</sup>	BU 86728 31399	28.1	56.6	15.2						256
	Tir Mala <sup>1</sup>	BU 90149 53013	60.4	38.5	1.1						273
Wadi ar-Rabiya	Motorway <sup>3</sup>	BU 93392 14769	11.6	85.2						3.2	250
	SE of Al Qusayr <sup>4</sup>	BU 80187 19083	12.9	87.1							255
Middle Orontes	Rastan <sup>5</sup>	BU 93451 66988	40.7	45.8						13.4	253
	Jnan <sup>6</sup>	CU 02201 85047	29.0	71.0							276
	Ain Kassarine <sup>7</sup>	CU 01128 88403	61.5	37.8			0.4			0.4	275
	Latamneh south <sup>8</sup>	BV 83384 09911	27.7	70.8			1.2			0.4	253
	Latamneh Lower <sup>9</sup>	BV 83022 10451	99.2	0.8							251
	Latamneh Upper <sup>10</sup>	BV 83021 10459	99.6			0.4					276
Ghab	Karkour sluice <sup>11</sup>	BV 57282 59073	96.6	3.4							268
Darkush	Gorge <sup>12</sup>	BV 63445 77174	0.7	99.3							149
Amik	Alaattin Köyü <sup>13</sup>	BA 52477 15506	9.8	73.9		0.7	10.1	3.1	0.4	1.8	287
Lower Orontes	Antakya bypass <sup>14</sup>	BA 41382 06943	0.4			1.1	29.8	51.6	14.4	2.9	285
	Şahin Tepesi <sup>15</sup>	BV 38313 99525	1.7	7.0		1.0	42.4	40.4	2.6	5.0	302

Notes:

1 – Voids probably represent dissolved limestone clasts

2 – See Fig. 4B

3 – Others are calcareous sandstone (2.4%) and marl (0.8%)

4 – Chert includes one worked flake

5 – Gravel also contains boulders of basalt, highly weathered; voids might represent smaller basalt clasts (weathered away) as well as dissolved limestones

6 – Basalt clasts are conspicuous at larger sizes

7 – Others = 1 x calcareous sandstone

8 – Sample was collected from a disused small quarry between Latamneh village and the River Orontes, at a lower level than and ~600 m southeast of the extant Latamneh quarry; the flint includes two worked flakes and four banded cherts of Upper Orontes type; others = 1 weathered bone fragment

9 – Sample was collected from the lower gravel in the extant Latamneh quarry; flint includes three worked flakes

10 – Sample was collected from the upper gravel in the extant Latamneh quarry; flint includes two worked flakes

11 – Flint includes four cherts of Upper Orontes type

12 – Undersized sample from valley-floor gravel beneath loam, collected at Hammam ash Sheykh Isa, between Jisr esh-Shugur and Darkush.

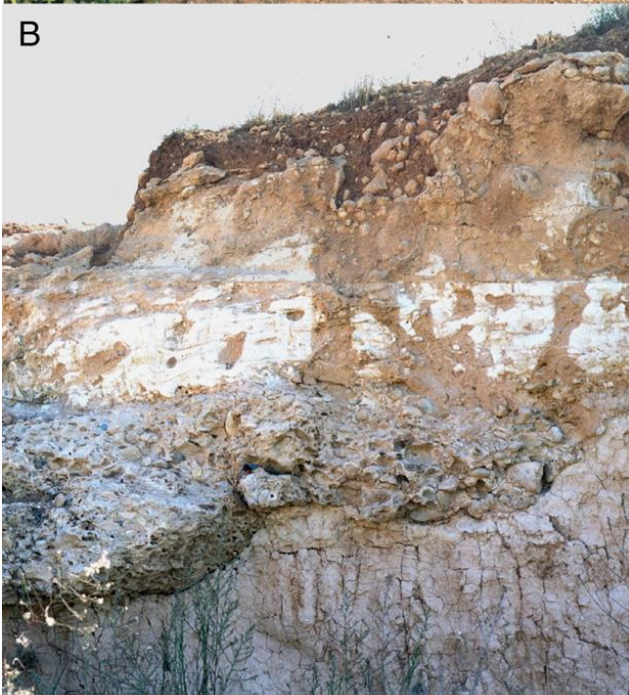
13 – Ophiolite includes a single clast of amphibolite; others includes two clasts of weathered schist and a single pottery fragment (?Roman or similar). The schist probably originated in the Amanos Mountains to the north, having been worked into the Amik Basin by the River Karasu. Other constituents of this gravel, such as limestone, quartzite and basalt, may have shared this provenance.

14 – Others are kaolinized crystalline rocks (2.5%) and a single vein quartz (0.4%)

15 – Sample collected from a flat overlooking the left bank of the Orontes apparently by a tributary deposit; others are weathered crystalline, perhaps related to ophiolite; ophiolites include chert (0.7%), weathered foliated rock (0.7%), schistose with serpentine (1.0%) and olivine-rich ultramafic (0.4%).

211  
212  
213  
214  
215  
216  
217  
218  
219  
220  
221  
222  
223  
224  
225  
226  
227  
228  
229  
230  
231  
232

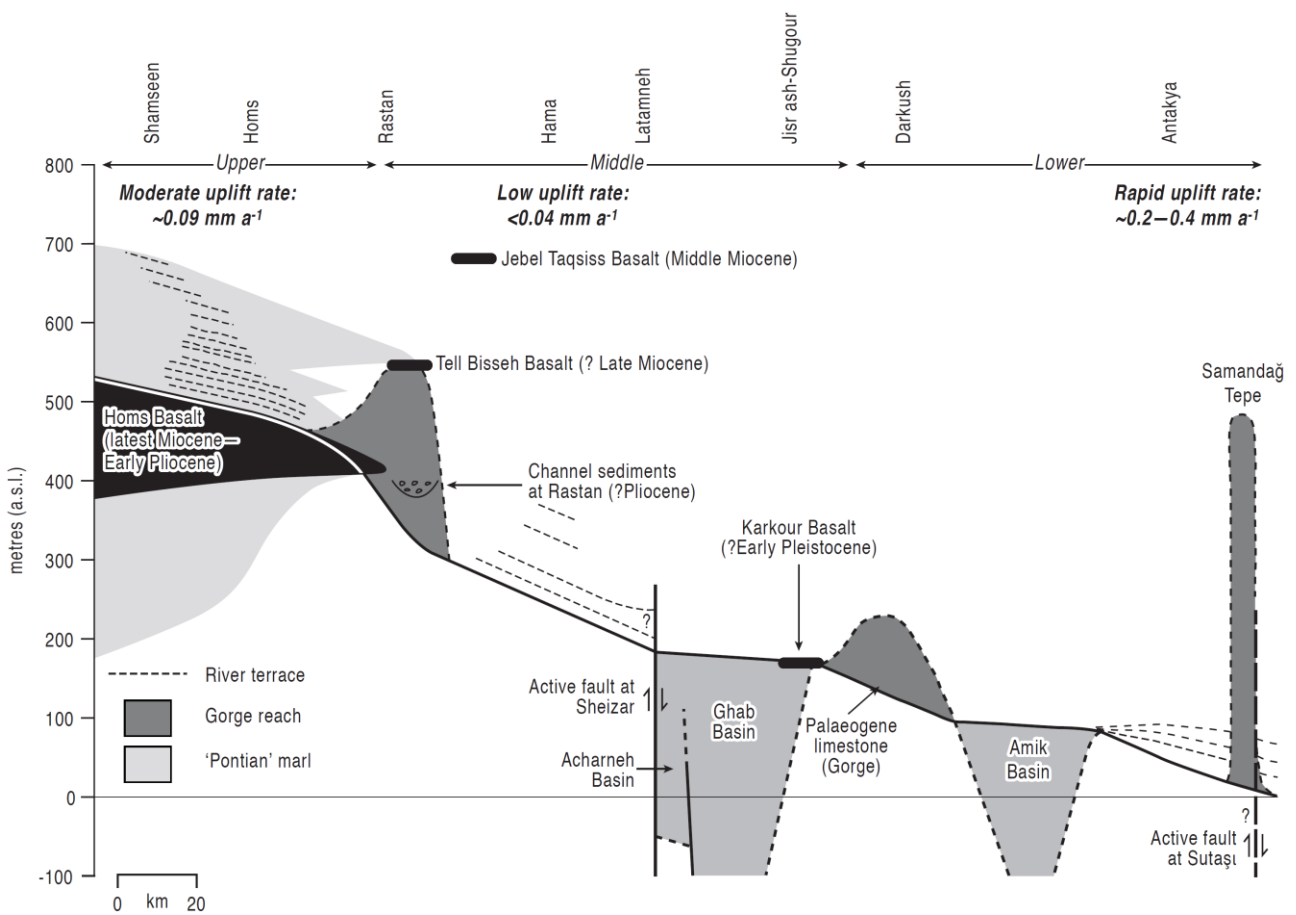
233 The Quaternary record of the Upper Orontes received little attention prior to the Homs Survey,  
 234 although Van Liere (1961) alluded to Neogene–Pleistocene conglomeratic sediments that he  
 235 attributed to braided fans; these can now be interpreted as (cemented) Quaternary river terrace  
 236 deposits (Bridgland et al., 2003; Bridgland and Westaway, 2008a; Fig. 2). The eastern valley side  
 237 of the Orontes in this region slopes gently from >750 m a.s.l. (above sea level) to river level at 480–  
 238 510 m, over a distance of ~15 km, within which is preserved an extensive sequence of Late  
 239 Cenozoic terraces (Fig. 4). In the marl areas these are represented by localized but conspicuous  
 240 chert/flint-rich conglomerates, densely cemented by carbonate, of the type noted by Van Liere  
 241 (1961); occasionally these record the three-dimensional form of fluvial channels (Fig. 2B), which  
 242 suggests that they represent ‘channel calcretes’ (cf. Wright and Tucker, 1991; Nash and Smith,  
 243 1998, 2003; McLaren, 2004). The conglomerates are rarely more than ~1 m thick, which has  
 244 allowed farmers to displace them from field surfaces to boundary lines or informal clearance cairns.



In situ conglomerates are seen in occasional quarry sections and road cuttings, or in surface outcrop amongst farmland where they have proved too difficult to remove; they are also seen frequently in the sides or beds of unpaved tracks, such outcrops having been the basis of much of the terrace mapping in the Upper Orontes (Bridgland et al., 2003). In exposure the conglomerates are seen to be interbedded with finer-grained alluvial sediments (Fig. 2B) in sequences showing fluvial bedding structures. The recognition of these conglomerates as Orontes terrace gravels is confirmed by the occurrence of the most extensively preserved conglomerate forming a low-level right-bank terrace (the al-Hauz Terrace), which can be traced for several kilometres beside the river upstream of Lake Qatina (Bridgland et al., 2003; Figs 1, 2C, 3 and 4). Sections in the cemented Orontes gravels show that their uppermost levels, especially where they are immediately below the land surface, have generally been decalcified, with prominent ‘pipe’ structures reaching depths of a metre or more (Fig. 2B; online supplement, Fig. A.1.1).

**Figure 2** –The Upper Orontes valley, field photograph: A- Typical exposure of cemented gravel in the land surface beside a rural road (at BU 75492 26442), showing the subdued relief of the Upper Orontes terrace staircase (looking northwards); this deposit is ~520 m a.s.l. and is interpreted as forming part of the Tir Mala terrace (Fig. 4; Table 2). B- Section at Arjun, showing lower cemented gravel filling a channel cut in (much softer) Pliocene marl bedrock, overlain by calcified fine-grained fluvial sediments, with post-depositional solution structures. The calcreted channel gravel illustrated here was sampled for U-series dating (see online Appendix 2). C- Cemented gravels of the lowest (al-Hauz) terrace of the Orontes, exposed in the right bank of the river at the type locality, ~25 km south-west of Homs.

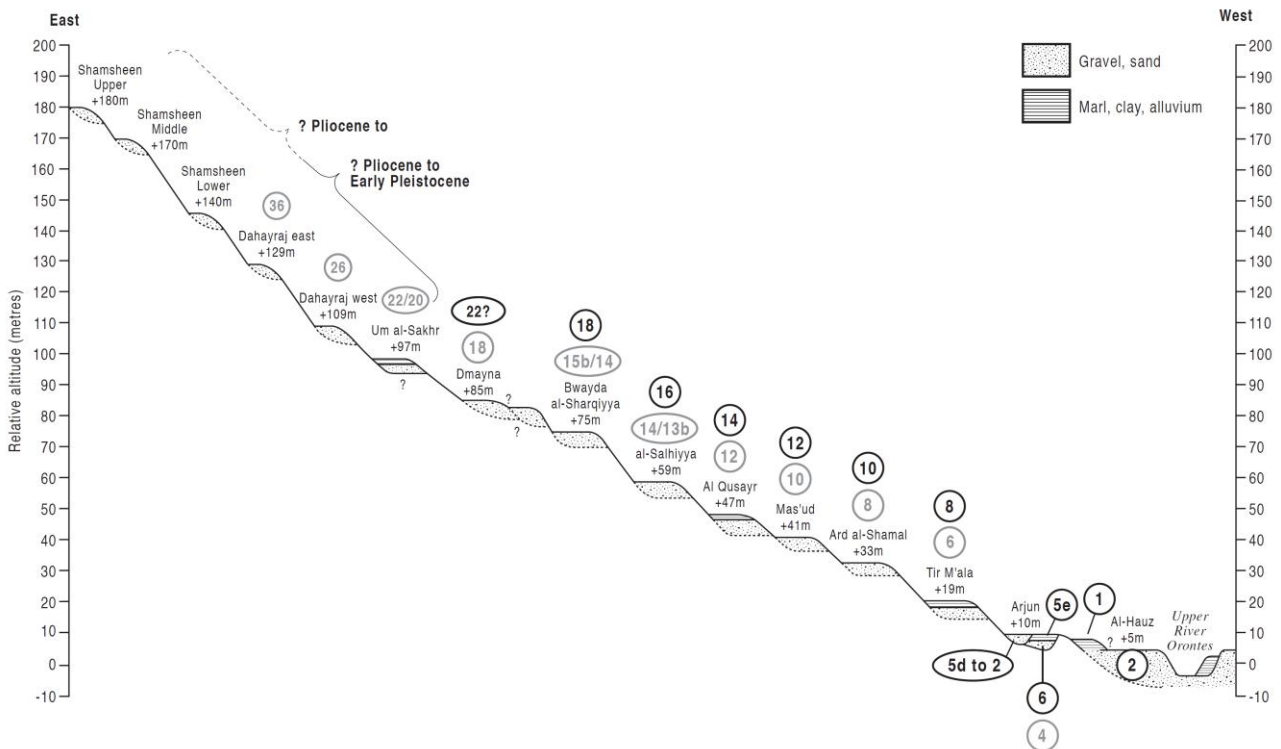
282 A single example of channel calcrite has been analysed in some detail, in part to determine the  
 283 potential for dating the calcite cement using the uranium-series method (e.g. Ivanovitch et al., 1992;  
 284 see below). Samples of the cemented channel-fill gravel at Arjun (Fig. 2B) were subjected to  
 285 petrological and geochemical analyses, which revealed evidence for two phases of calcite cement  
 286 precipitation. The first, fine grained and brown in colour, was restricted to occasional and  
 287 sometimes fragmentary pebble coatings, only intermittently present and lacking any preferred  
 288 orientation. The second, in contrast, was pinkish grey and filled interstices within a clast-supported  
 289 sandy, silty matrix, thus forming the bulk of the calcrite cement (see online Appendix 2). The  
 290 fabric of the conglomerates forming the higher (and therefore older) terraces has been considerably  
 291 modified by repeated decalcification and re-cementation; clasts (presumably calcareous ones) have  
 292 been weathered out to leave cavities, sometimes partly filled with re-precipitated calcium carbonate.  
 293 This means that the fluvial bedding structures are best preserved in the younger conglomerates,  
 294 such as those forming the Arjun and al-Hauz terraces (Figs 2C and 4).



295  
 296 **Fig. 3** Long profiles of the Orontes valley floor and its terraces in relation to gorge reaches, subsiding fluvio-lacustrine basins and basalt flows.  
 297 Summaries of pos-Early Pleistocene histories of the terraced reaches are also shown (for explanation, see text).

298 Bridgland et al. (2003) reported Orontes terrace deposits at up to 130 m above the modern river  
 299 (Table 2). They constructed an age model for this sequence, assuming climatically generated

300 terrace formation in approximate synchrony with 100 ka (Milankovitch) climatic fluctuation (cf.  
 301 Bridgland, 2000; Bridgland and Westaway, 2008a) and using a correlation, based upon height  
 302 above the modern river, with the sequence in the Middle Orontes, for which there is vertebrate  
 303 biostratigraphical evidence (see below). Further consideration of the palaeontological evidence,  
 304 however, indicates that the age model used in 2003 was a significant underestimate (see below).  
 305 Subsequent attempted U-series dating of the Arjun channel calcrete (see above) has provided an  
 306 adjusted age pinning point for the Upper Orontes terrace staircase, albeit rather low in the sequence.  
 307 Different U-series age estimates were obtained for the brown pebble coatings and the pinkish-grey  
 308 interstitial cement: >350,000 years for the former and  $155,000 \pm 17,000$  years for the latter (see  
 309 online Appendix 2). The pebble coatings are interpreted as reworked older cement that was already  
 310 present on clasts derived from older gravels within the sequence. It is considered, therefore, that the  
 311 age of the interstitial cement is more representative of the channel gravel. It should be noted that  
 312 channel calcretes form in active (semi-arid) fluvial environments, by infiltration of calcareous water  
 313 into recently deposited underlying sediment, so there is every reason to believe that the cement was  
 314 precipitated during the same geological episode as the gravel (cf. Nash and McLaren, 2003;  
 315 McLaren, 2004).



316  
 317 **Fig. 4.** Idealized transverse section through the terrace sequence upstream from Homs (after Bridgland et al., 2003, with modifications). MIS  
 318 attributions suggested by Bridgland et al. (2003) are shown, together with the older correlations now suggested (see text).

319 The basal channel gravel at Arjun is thus attributed to Marine oxygen Isotope Stage (MIS) 6, rather  
 320 than the MIS 4 age favoured by Bridgland et al. (2003). A comparison of the earlier 2003 and

321 revised age models is provided by Figure 4. An important implication of the revision is that uplift  
 322 has been significantly less rapid than previously supposed: 85 m since MIS 22, instead of 97 m (see  
 323 Fig. 4).

324 Fieldwork in 2002–3, reported here for the first time, has revealed that the Upper Orontes terrace  
 325 staircase extends higher than was reported by Bridgland et al. (2003), the highest gravel remnants  
 326 being found in cuttings along the Homs–Damascus motorway as it crosses the interfluvium between  
 327 the Orontes and its prominent tributary, the Wadi ar-Rabiya (Fig. 1). The oldest gravels occur in  
 328 the vicinity of Shamseen (at BU 925240), the highest being south of the village (BU 2930 3821),  
 329 ~700 m a.s.l. and ~180 m above the level of the modern Orontes (Fig. 4). Mapping of in situ fluvial  
 330 conglomerates has revealed at least fifteen Upper Orontes terraces (Figs 3 and 4), although the  
 331 wider vertical gaps between the higher terrace remnants suggest that others await discovery or have  
 332 been removed by erosion.

333 **Table 2** Upper Orontes terrace stratotypes and other key localities, numbered sequentially. To obtain accurate positioning, co-ordinates of sites were  
 334 measured in the field using a portable GPS receiver, and are expressed as 8- or 10-digit grid references using the Universal Transverse Mercator  
 335 (UTM) system. Height information has been obtained from dGPS and/or SRTM topographic imagery.

<b>Terrace</b>	<b>Type locality (UTM Coordinates)</b>	<b>Above river</b>	<b>Height a.s.l.</b>	<b>MIS 2003<sup>1</sup></b>	<b>Revised MIS</b>
<b>al-Hauz</b>	Right bank of the Orontes (BU 7345 2783)	5 m	506 m	2	2
<b>Arjun</b>	Quarry (BU 7458 2573)	10 m	512 m	5d-2	6-2
<b>Tir M'ala</b>	Bluff exposure (BU 9023 5296)	19 m	471 m	6	8
<b>Ard al-Shamal</b>	Surface exposure (BU 7762 2598)	33 m	534 m	8	10
<b>Mas'ud</b>	Surface exposure (BU 7877 2570)	41 m	542 m	10	12
<b>Al Qusayr</b>	Surface exposure (BU 7918 2288)	47 m	551 m	12	14
<b>al-Salhiyya</b>	Surface exposure (BU 8209 2876)	59 m	552 m	14 or 13b	16
<b>Bwayda al-Sharqiyya</b>	Surface exposure (BU 8482 3052)	75 m	567 m	16 or 15b	18
<b>Dmayna</b>	Bluff exposure (BU 8512 2897)	85 m	580 m	18	?22
<b>Um al-Sakhr</b>	Quarry (BU 8673 3142)	97 m	584 m	22 or 20	–
<b>Dahayraj West</b>	Surface exposure (BU 8537 2249)	109 m	613 m	26	–
<b>Dahayraj East</b>	Surface exposure (BU 8846 2614)	129 m	625 m	36	–
<b>Shamseen Lower</b>	Surface exposure (BU 91260 28896)	~140 m	637 m	–	–
<b>Shamseen Middle</b>	Surface exposure (BU 92897 22448)	~170 m	689 m	–	–
<b>Shamseen Upper</b>	Surface exposure (BU 93026 21473)	~180 m	698 m	–	–

336 Notes: 1 – MIS correlations proposed by Bridgland et al. (2003). Information from more recent research suggests that ages have been underestimated  
 337 (see revised MIS column)  
 338

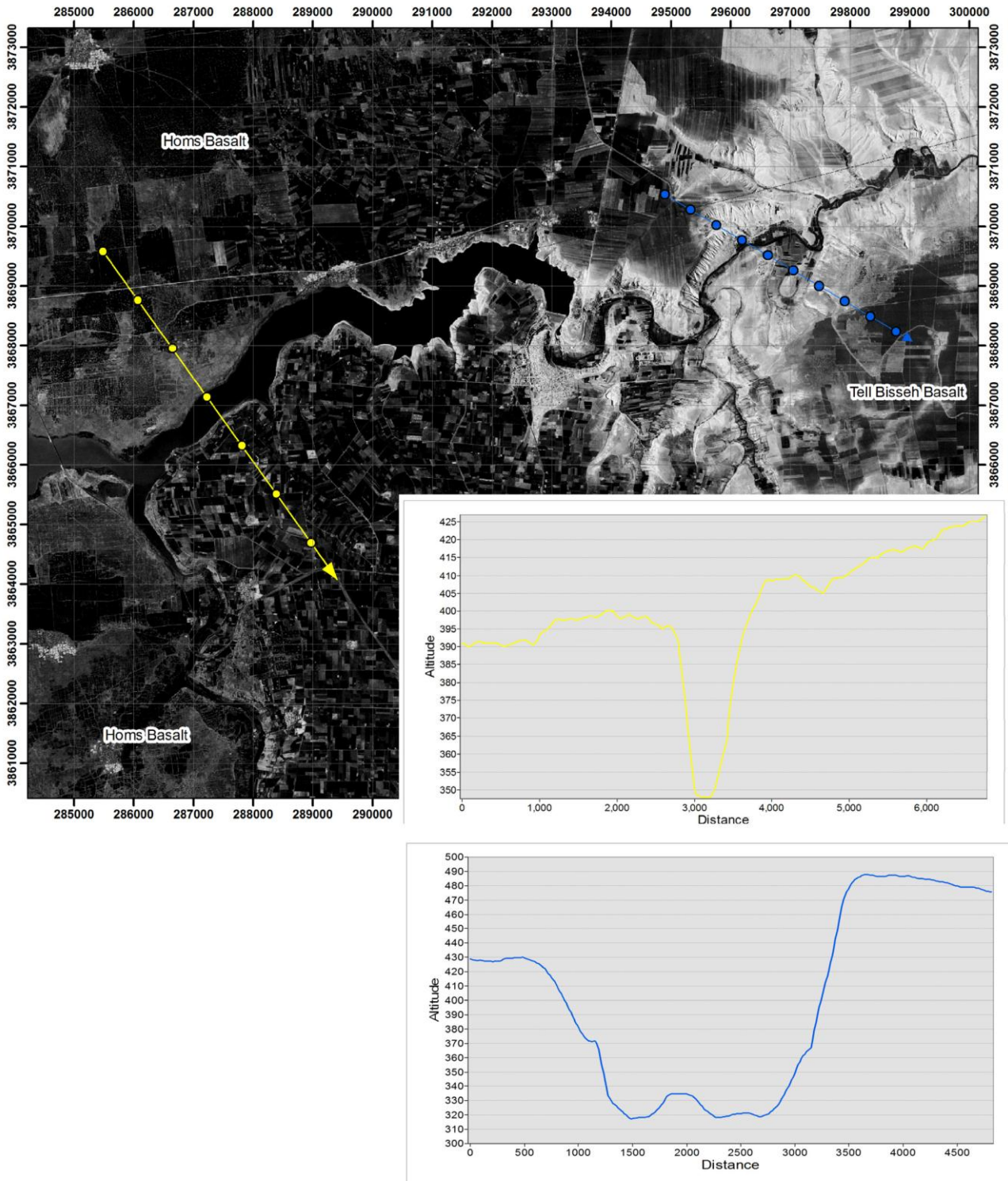
339 The Upper Orontes gravels are characterized by two main rudaceous components: (1) flint and/or  
 340 chert, highly variable in character, and (2) limestone. The siliceous rocks are believed to have been  
 341 derived both from the valley sides (from Cretaceous and Palaeogene flint-bearing strata) and from  
 342 upstream in the Orontes catchment, whereas the limestone probably represents Cretaceous–Miocene

343 occurrences in the wider region (e.g. Ponikarov et al., 1963a). The limestone component varies  
344 from approximately one third of the (16–32 mm) total to nearly three-quarters (counting voids as  
345 limestone clasts removed by solution: see above and Table 1). Thus the siliceous lithologies never  
346 fall below 25% of the total count in those Orontes gravels analysed (Table 1). Substantial gravels  
347 have also been produced by the Wadi ar-Rabiya (Fig. 1); calcreted gravels, presumably from the  
348 last climate cycle, are well exposed in a wadi-floor quarry (BU 85311 19993). These wadi gravels,  
349 however, are invariably dominated by limestone clasts, although up to 14% flint/chert occurs in  
350 them (Table 1), presumably reworked from the older Orontes terraces, across which the tributary  
351 has flowed. Thus, clast analyses can be used as a means of recognizing the deposits of the main  
352 river, with their larger siliceous component.

#### 353 **4. The Rastan Gorge**

354 The gorge at Rastan reflects the lateral constriction of the river in its passage through the relatively  
355 resistant Homs Basalt. The puzzling disposition of the gorge close to the eastern margin of the  
356 basalt outcrop (Fig. 5) suggests that the course of the Orontes here has been superimposed from a  
357 valley originally developed in less resistant overlying marl. Indeed, the basalt is known from  
358 borehole data (Ponikarov et al., 1963a) to have an eastward inclination, which suggests that its  
359 exhumation from beneath overlying marl will have caused the cessation of the westward migration  
360 of the river exemplified by the distribution of terraces further upstream. Geological mapping  
361 (Ponikarov et al., 1963a) indicates that a flow unit of Homs Basalt reached the Rastan area from the  
362 main outcrop west of the Orontes valley. Its main outcrop, on the north side of the valley, reaches a  
363 location ~2 km north-east of Rastan (~ BU 940700), where its upper surface is ~420 m a.s.l., dying  
364 out just east of the point where the gorge is crossed by the Damascus–Aleppo motorway viaduct. A  
365 smaller basalt outcrop south of the river, also depicted on the 1963 geological map, reaches ~1 km  
366 west of Rastan (~ BU 920680), where it is ~400 m a.s.l. This outcrop is both overlain and underlain  
367 by the ‘Pontian’ marl; however, the overlying marl is locally no more than a few tens of metres  
368 thick, although its above-basalt thickness increases southwards to ~100 m in the Homs area (Fig. 3),  
369 according to borehole data compiled by Ponikarov et al. (1963a). The larger outcrop on the north  
370 side of the valley is underlain by the marl, but any overlying marl has been lost to erosion. The  
371 Orontes is locally ~320 m a.s.l.; the ~100 m depth of the Rastan Gorge below the top of the basalt  
372 and overlying marl, determined from GIS data (Fig. 5), thus provides a measure for fluvial incision  
373 in the ~4–5 million years since the basalt eruption and cessation of marl deposition. Fluvial  
374 deposits reported by Bridgland et al. (2003) in the southern approach cutting to the Rastan  
375 motorway viaduct (online supplement, Fig. A.1.2) are at roughly the same height as the basalt south

376 of the river and thus (rather than the early Middle Pleistocene age previously suggested) probably  
 377 indicate the Early Pliocene level of the Orontes.



378

379 **Fig. 5.** The Rastan Gorge. This is a CORONA image from the 1960s, with derived transverse profiles (colour coded). Positions of the two basalts, of  
 380 different age, are indicated (see text). The westernmost (upper) cross section is located on the Homs Basalt on both sides of the river, whereas the  
 381 easternmost (lower) cross section shows the higher Tell Bisseh Plateau on the right bank of the river.

382 On the southern side of the river, ~4–12 km downstream of Rastan, an older basalt has been  
 383 exhumed from beneath the marl to form the capping of the Tell Bisseh Plateau (Figs 3 and 5), up to

384 550 m a.s.l.; it is mapped as Upper Miocene (Ponikarov et al., 1963a), although it has not been  
385 dated directly. Furthermore, higher-level basalts further downstream, in the Middle Orontes, have  
386 yielded Middle Miocene ages (Sharkov et al., 1994; see below).



**Fig. 6.** Terraces of the Middle Orontes: A- View looking downstream from CU 02087 83210, a location on the inside of a meander loop on the left (west) side of the Orontes, ~10 km south-east of Hama. Landforms on this side of the valley hereabouts were mapped by the French as part of their numbered ‘glacis’ and terrace system but clearly developed in bedrock, rather than being a depositional features (see text). On the right skyline is a basalt-capped mesa (a volcano), which is ~10 km distant, with its summit at CU 034927. B- Surface exposure in cemented gravel at CU 09511 78980, ~410 m a.s.l. (>100 m above modern river level). The view is northward, looking across the valley of an Orontes tributary, the Wadi Kafat, towards the basalt-capped plateau in the distance, from a point ~3 km east of the modern river. C- Limestone fan gravels at the Khattab 2 locality (see also online supplement, Fig. A.1.4; see text for explanation). The gravels are exposed in the bluffs beneath the building on the skyline.

## 5. Middle Orontes: Rastan to the Ghab Basin

For much of its length, the Middle Orontes forms a deep valley up to 400 m below a succession of flat-topped hills capped with basalt mapped as Upper Miocene (comparable with that capping the Tell Bisseh Plateau, noted above: Ponikarov, 1986); the highest of these, Jebel Abou Dardeh and Jebel Taqsiss, reach 682 and 685 m a.s.l., according to Besançon and Sanlaville (1993a). The river loops east of Jebel Taqsiss, north of Rastan, and then turns northwards, flowing to the west of other mesas in the area north and east of Hama

419 (see Fig. 6A and B). Sharkov et al. (1994) obtained whole-rock K–Ar dates of  $17.3\pm 0.6$  and  
420  $12.8\pm 0.6$  Ma for basalt samples from Jebel Taqsiss, implying eruption in the Middle rather than the  
421 Late Miocene, as well as  $12.0\pm 0.5$ ,  $10.8\pm 0.3$ , and  $7.8\pm 0.3$  Ma for basalt samples from the area

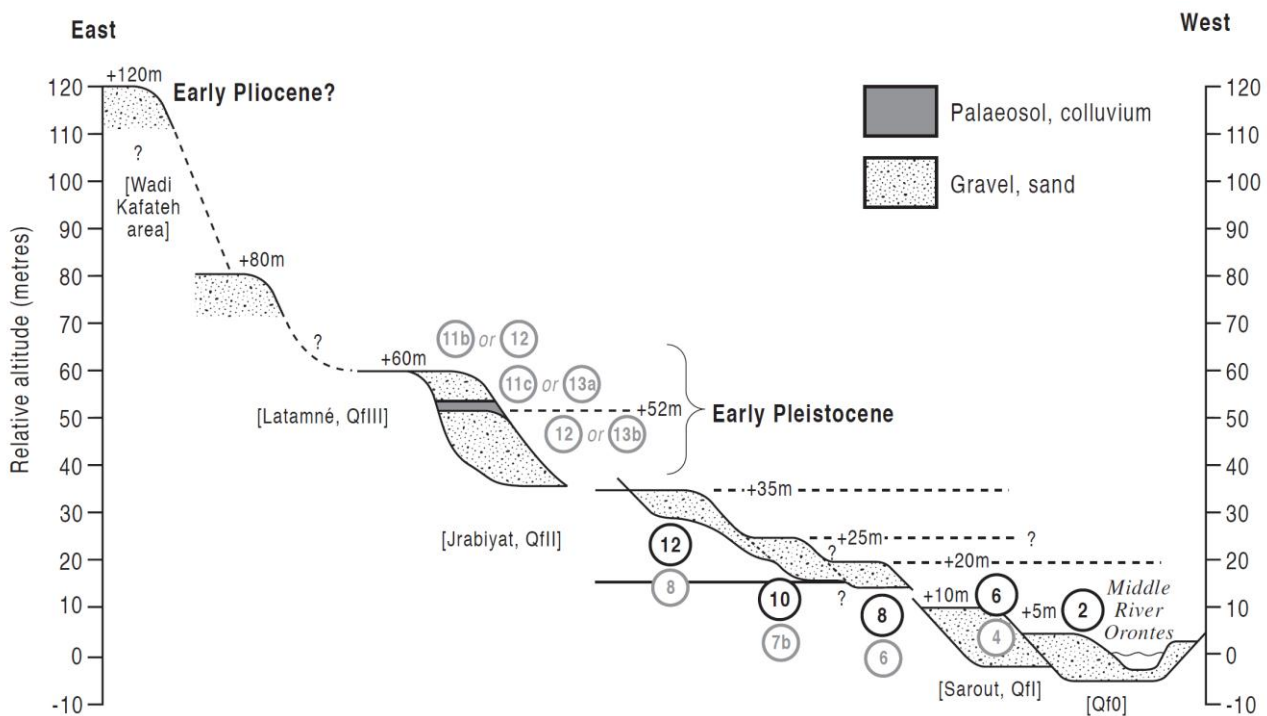
422 north-east of Hama. It is now apparent, however, that K–Ar dates of this whole-rock type  
423 frequently result in numerical ages that are significantly older than the true age of the volcanism, as  
424 a result of inherited argon in phenocrysts (Kelley, 2002); this problem, noted above in relation to  
425 the Homs Basalt (Westaway, 2011), raises doubts about the accuracy of the above ages.  
426 Nonetheless, it is apparent, from its relation with the Pontian lacustrine marl, that the Tell Bisseh  
427 Plateau Basalt is older than the latest Miocene–Early Pliocene Homs Basalt. It is also clear that  
428 the basalts capping Jebel Taqsiss and the mesas north and east of Hama (also mapped as Upper  
429 Miocene) belong to the older group, although determining whether they represent a single eruptive  
430 phase must await future dating. Bridgland et al. (2003) were thus incorrect in their correlation of  
431 the Jebel Taqsiss and Homs basalts, with the inference that the whole ~400 m of entrenchment of  
432 the Middle Orontes had developed since the Early Pleistocene. On the contrary, it is now clear that  
433 the Middle Orontes valley is of much greater antiquity, apparently dating back at least to the Middle  
434 Miocene, with the implication that fluvial incision has been correspondingly slower than was  
435 previously supposed. The basalt-capped mesas of the Middle Orontes valley are formed in  
436 Palaeocene–Eocene nummulitic limestones, lying to the north of the latest Miocene lacustrine basin  
437 (Van Liere, 1961).

438 The fluvial sediments of the Middle Orontes have been studied since the early 1930s (Burkhalter  
439 1933), although a major catalyst for research in this area was the discovery of an extensive  
440 mammalian fossil assemblage in gravel quarries ~1.5 km south of the village of Latamneh (Van  
441 Liere, 1960; Hooijer, 1961, 1965; Fig. 1; see below). This led to a series of excavations in which  
442 unabraded Lower Palaeolithic artefacts were recovered from fine-grained fluvial deposits overlying  
443 the gravels containing the vertebrate fauna (e.g., Modderman, 1964; Clark, 1967, 1968). Latamneh  
444 is the single major source of fossils in the Middle Orontes and provided the vertebrate  
445 biostratigraphical evidence used by Bridgland et al. (2003), by extrapolation upstream, as an age  
446 indicator for their Upper Orontes sequence (see above). In addition, a tooth of the ancestral  
447 mammoth *Mammuthus meridionalis* was reported from a gravel quarry at Sharia, east of Hama  
448 (Van Liere and Hooijer, 1961), in an area subsequently built over during the expansion of the city.  
449 This contrasts with the teeth of the more evolved mammoth *Mammuthus trogontherii* from  
450 Latamneh (e.g. Van Liere, 1960; Hooijer, 1961, 1965), ~25 km downstream of Hama (Fig. 1).

451 During the late 1970s and early '80s a team from the French Centre National de la Recherche  
452 Scientifique (CNRS) instigated a survey of Pleistocene deposits in the Middle Orontes valley in  
453 order to place the discoveries from Latamneh within a local chronostratigraphical sequence  
454 (Besançon et al., 1978a, b; Besançon and Sanlaville, 1993a; Copeland and Hours, 1993). This led

455 to the discovery of Lower and Middle Palaeolithic artefacts at a number of localities and the  
 456 identification of a sequence, above the valley-floor alluvium, of up to five terraces, as follows (from  
 457 Besançon and Sanlaville, 1993a):

- 458 Qf0 Floodplain and Holocene alluvium of the valley bottom
- 459 QfI Lowest Pleistocene terrace; ~10 m above river
- 460 Qf II Second Pleistocene terrace; ~25 m above river
- 461 QfIII Third Pleistocene terrace; includes Latamneh; 30–60 m above river
- 462 QfIV Fourth Pleistocene terrace; ~80 m above river
- 463 QfV Highest Pleistocene terrace
- 464 (Note: the ‘f’, for fluvial, as opposed to ‘m’ for marine, was not always used)



466 **Fig. 7.** Idealized transverse section through the terrace sequence of the Hama–Latamneh area, showing the MIS correlation suggested by Bridgland et  
 467 al. (2003), now thought to be underestimated, and the greater ages suggested in this paper (see text). Uses data from Besançon and Sanlaville (1993a)  
 468 and Dodonov et al., (1993); artwork modified from Bridgland et al. (2003).

469 The CNRS team mapped these five terraces along the Orontes from the Rastan Gorge to the  
 470 southern end of the Ghab Basin, with preservation distributed on both sides of the valley, although  
 471 QfV was identified as an erosion surface that was devoid of fluvial sediments and QfIV was  
 472 mapped as a ‘glacis’ with occasional (poorly documented) traces of fluvial conglomerate.  
 473 Fieldwork during 2007 and 2009 has shown the CNRS feature mapping to be generally sound but,  
 474 whereas the right-bank terraces are generally formed from fluvial gravels and floodplain silts, those  
 475 on the left bank (including those below QfIV) are often ‘glacis’ type features formed in bedrock or

476 slope deposits and incorporating valley-side fans and colluvial slope aprons (Fig. 6.A). It was also  
477 found that the terrace sequence in this reach extends higher above the river on the eastern side of the  
478 valley than had been realised previously, with a series of cemented gravels capping hills southeast  
479 of Hama and west of Salamiyeh (Figs 1, 6B and 7). The highest level at which ancient Orontes  
480 sediments have been observed hereabouts is alongside its right-bank tributary, the Wadi Kafateh,  
481 which joins the main river some 8 km upstream of Hama (online supplement, Fig. A.1.3). These  
482 cemented gravels, which crop out widely hereabouts, can be confirmed as Orontes deposits from  
483 their flint content; in every respect, including their disposition within the landscape, they resemble  
484 the high-level conglomerates of the reach above Homs. There are several facets underlain by  
485 gravel, the highest reaching 410 m a.s.l. (Fig. 6B), with lower-level 'flats' down to a prominent  
486 level at ~370 m a.s.l., well developed around CU 08825 81661. The sequence thus ranges between  
487 80 and 120 m above the modern level of the river (Fig. 7). Whether these are erosional facets or  
488 whether they mark 'cut-and-fill' events cannot be determined.

489 The height of these cemented gravels, in comparison with the fossiliferous deposits at Latamneh  
490 (see below), helps confirm the great antiquity of Orontes drainage in north-western Syria and their  
491 disposition implies westward migration of the river during the Late Cenozoic, helping to explain the  
492 absence of fluvial terrace deposits on the left bank of the river. On the basis of height above the  
493 river, bearing in mind the disposition of the fluvial deposits at Rastan (see above), an Early Pliocene  
494 age is tentatively estimated for these high-level deposits of the Middle Orontes.

495 In contrast to these new discoveries, the single locality at which the French workers recorded  
496 substantial gravels beneath their QfIV terrace, Khattab 2 (regarded by them as the type locality of  
497 the Khattabian Palaeolithic Industry: Copeland and Hours 1993; location: BU 88795 96553), was  
498 visited in 2007 and found to expose a cemented limestone gravel of presumed local, perhaps  
499 alluvial-fan origin. It comprises mainly rounded limestone pebbles, although with large angular  
500 flints that have clearly not been subjected to significant fluvial transport. Thus, despite occurring in  
501 the flanks of a steeply incised reach of the Orontes, this deposit must be rejected as a product of that  
502 river, since all Orontes gravels in the Middle reach are strongly dominated by subangular siliceous  
503 clasts. Indeed, the location of the cemented gravel adjoins a confluence with a tributary wadi (cf.  
504 Besançon and Sanlaville, 1993a, their figure 7A), which is the possible source of the material. This  
505 interpretation is supported by the poorly stratified nature of the deposit, more akin to fan gravel than  
506 a fluvial channel facies (Fig. 6C; online supplement, Fig. A.1.4). Besançon and Sanlaville (1993a)  
507 regarded the Khattab gravel as older than the QfIII deposits encountered at Latamneh and  
508 elsewhere, largely because the former is well-cemented, whereas the QfIII deposits of the Middle

509 Orontes are not; its height, no more than ~30 m above the modern river, is not a basis for  
510 considering it as ancient. The cemented nature of the deposit, however, can probably be attributed  
511 to its limestone clast composition, since evidence from other reaches of the Orontes shows that in  
512 calcareous groundwater areas gravels can be cemented rapidly, as in the lowest terraces of the  
513 valley upstream from Homs (see above).

514 Copeland and Hours (1993) applied the name Khattabian to a series of artefact assemblages lacking  
515 handaxes that they considered older than those from handaxe-bearing QfIII terrace deposits such as  
516 at Latamneh. This material was reportedly from pockets of fluvial conglomerate on the QfIV  
517 terrace glacia, some of which were at much greater heights than the supposed type locality at  
518 Khattab. Recent re-examination of the artefacts from the type locality at Khattab (Shaw, 2008, in  
519 press) failed to identify any pieces unequivocally of human manufacture, nor indeed were any  
520 definite artefacts identified amongst the small collections from the five other 'Khattabian' findspots  
521 in the Orontes (Abu Obeida, Mahardeh 2, Ard Habibeh, el-Farcheh 1 and Khor el-Aassi). Not only  
522 is the age attribution of the Khattab 2 type locality suspect, therefore, but the status of a separate  
523 and earlier non-handaxe industry is also open to question, particularly since handaxes are known  
524 from the site at Ubeidiya, further south in the Levant, in deposits dating from the mid Early  
525 Pleistocene, ~1.4 Ma (Tchernov, 1987, 1999). The only one of these 'Khattabian' sites that is both  
526 at a relatively high level and, from the brief descriptions by Besançon and Sanlaville (1993a) and  
527 Copeland and Hours (1993), clearly in deposits of the Orontes, is el-Farcheh (~CU 045 850); at  
528 ~340 m a.s.l. it is ~55 m above the river. Being significantly lower, this is evidently younger than  
529 the gravels described above in the vicinity of the Wadi Kafateh; the deposits at el-Farcheh can be  
530 tentatively ascribed to the latest Pliocene–earliest Pleistocene.

531 The aforementioned Latamneh locality in fact constitutes a number of separate sites (Fig. 8) that  
532 were worked for gravel during the latter half of the 20<sup>th</sup> and into the present century, details of  
533 which have been reviewed recently by Shaw (2008, in press). Remote sensing data from different  
534 dates has now been used to determine the disposition of the sediments. In summary of these various  
535 findings, it has been concluded that the large extant quarry (online supplement, Fig. A.1.5) studied  
536 by the present authors is an expanded version of what was called Latamneh 2 by Copeland and  
537 Hours (1993); it is, however, a later working than was available in the 1960s, when bulk of the  
538 collections were made (Clark, 1966a, b; Van Liere, 1966; de Heinzelin, 1968) at localities 1–1.5 km  
539 to the south and east (Fig. 8). Much of the recorded mammalian material came from Latamneh  
540 Quarry 1 (Hooijer, 1961, Van Liere, 1966) and from two sondages (A and B) to the south. There  
541 were also finds from the working that Van Liere (1966) described as Quarry 2 (not the extant  
542 quarry) and from excavations (the 'Living Floor excavations') to the east of that quarry (Hooijer,

543 1965; Clark 1966a, b, 1967, 1968; see Fig. 8C), although they represent a small proportion of the  
544 total. The thick gravel sequence exposed in the extant quarry, mapped as QfIII (see above), is  
545 disposed between ~260 m and ~280 m a.s.l., the upper level being ~55 m above the level of the  
546 modern River Orontes, with a further ~10 m of silt above the quarried levels. There is nothing to  
547 contradict the view that all the various sites have exposed the same set of mammal-bearing fluvial  
548 deposits, these being the ‘lower gravels’ within the thick aggradational sequence here (cf. Shaw, in  
549 press).

## 550 **5.1 Biostratigraphical evidence from the Middle Orontes**

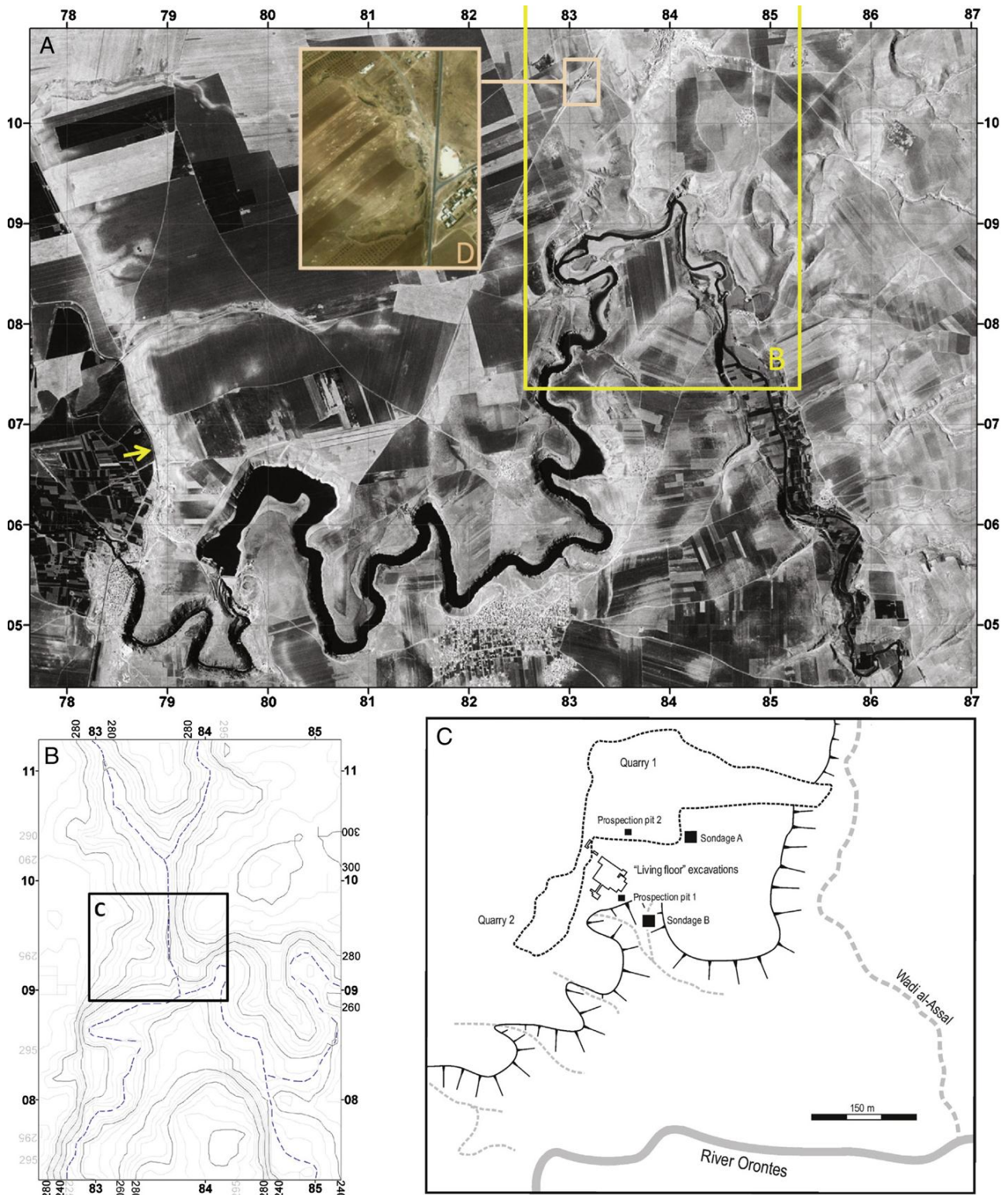
551 The mammalian remains from Latamneh include *Crocota crocuta*, *Hippopotamus* cf. *behemoth*,  
552 *Camelus* sp., *Giraffa camelopardalis*, *Praemegaceros verticornis*, *Bos primigenius*, *Bison priscus*,  
553 Bovidae de type antilope, gen. et sp. indet., cf. *Pontoceros* (?), *Equus* cf. *altidens*, *Stephanorhinus*  
554 *hemitoechus*, *Mammuthus trogontherii* and *Stegodon* cf. *trigonocephalus* (Guérin and Faure, 1988;  
555 Guérin et al., 1993). During the 2007 field season further vertebrate fossils were obtained from  
556 exposures in the large extant Latamneh quarry (see online supplement, Figure A.1.6), as follows:

- 557 1. Indeterminate bone fragment, white–pale yellow preservation, heavily weathered
- 558 2. Distal diaphysis of right humerus of fallow deer *Dama* sp. (probably *mesopotamica*)
- 559 3. Molar fragment (very crushed) of cf. *Stegodon* sp., encrusted with gravel
- 560 4. Left upper molar fragment of *Equus* sp.

561 These new discoveries contribute little to the list reported by Guérin et al. (1993); *Dama* cf.  
562 *mesopotamica* was recorded previously, along with *Camelus* cf. *dromedaries* and a molar  
563 tentatively attributed to *Gazella soemmering*, from the ‘Living floor’ excavations (Hooijer, 1965;  
564 Fig. 8C).

565  
566 The Latamneh assemblage is of Lower–Middle Pleistocene affinity and combines mammoth and  
567 giant deer species that are unknown in Europe after the Elsterian (excluding the dwarf form of *M.*  
568 *trogontherii* that characterizes MIS 7 faunas: Lister and Sher, 2001) with a rhinoceros (*S.*  
569 *hemitoechus*) that first appears in Europe immediately after that glacial, in the Holsteinian. On that  
570 basis Bridgland et al. (2003) suggested correlation with MIS 13 or 11 (perhaps a MIS 12 refugial  
571 population would be equally likely), considering this to be an important pinning point for Terrace  
572 QfIII within the Orontes sequence and for their uplift–incision modelling. There are, however,  
573 reasons to doubt that interpretation, which owed much to the occurrence of *S. hemitoechus*. In a  
574 recent review of Early and Middle Pleistocene faunas and archaeological evidence in the wider

575 region, Bar-Yosef and Belmaker (2010) have grouped Latamneh, despite the occurrence of *S. cf.*



576  
577 **Fig. 8.** The important archaeological and fossiliferous locality at Latamneh: A- CORONA image from the 1960s of the area between Latamneh and  
578 the Sheizar fault scarp, the latter being indicated with an arrow (top left); the southern part of Latamneh village is at the northern edge of this image,  
579 within the area of B. B- Contour map (5 m interval) derived from Shuttle Radar Topographic Mission (SRTM). C- Location of the earlier  
580 palaeontological and archaeological localities at Latamneh (from Shaw, in press). D- Inset showing a modern Google Earth view of the extant quarry  
581 at Latamneh, to the north of the earlier localities depicted in C.

582 *hemitoechus*, with a group of sites thought to represent the interval 1.2–1.0 Ma. In this they were  
583 influenced by the small mammal assemblage, in which Mein and Besançon (1993) reported the

584 arvicolid *Lagurodon arankae*, which is not thought to have survived into the Middle Pleistocene.  
585 Mein and Besançon (op cit) noted that all the small-mammal genera at Latamneh are represented at  
586 Ubeidiya, but by different species or more primitive morphotypes. The most abundant species at  
587 Latamneh is a gerbil, *Meriones maghrebianus*, which is defined on the basis of North African  
588 material. The species recorded as *Arvicola jordanica* is now attributed to a different genus,  
589 *Tibericola jordanica* Haas 1966, which is also present at Ubeidiya (Koenigswald et al. 1992) and  
590 Gesher Benot Yaaqov (Goren-Inbar et al. 2000), which, respectively, pre-date and post-date the  
591 supposed age of Latamneh (Bar-Yosef and Belmaker, 2010). *L. arankae* is indeed the most  
592 significant element, biostratigraphically; it first appeared in late Early Pleistocene Biharian faunas  
593 in eastern Europe but had disappeared by the early Middle Pleistocene (Markova, 2007), one of its  
594 last appearances being in the Karapürçek Formation in Turkey (Ünay et al., 1995, 2001; Demir et  
595 al., 2004), which is dated to ~ 0.9 Ma.

596

597 The location of the earlier discovery of a mandible, with teeth, of *M. meridionalis* at Sharia, near  
598 Hama (see above), also coincides with deposits mapped as QfIII by the CNRS workers, although in  
599 the original description Van Liere and Hooijer (1961) regarded it as older. This would seem to  
600 relate, at least in part, to the fact that Van Liere (1966) underestimated the height of the deposits at  
601 Latamneh. Artefacts were also discovered but the assemblage is too small for the absence of  
602 evidence for handaxe making to be meaningful. This leaves a conundrum in that ancestral  
603 mammoths of different types, and presumed to be at different evolutionary stages, are recorded in  
604 deposits that have been attributed to the same Orontes terrace. In an attempt to resolve this  
605 problem, the photographs of mammoth teeth provided for Sharia by Van Liere and Hooijer (1961)  
606 and for Latamneh by Hooijer (1965) were re-examined. This confirmed that the single R m3 tooth  
607 from Latamneh figured by Hooijer (1965) is consistent with an identification of *Mammuthus*  
608 *trogotherii*. Sixteen plates are apparent on the image but there has been a limited amount of wear  
609 at the front of the tooth so this should be regarded as a minimum count. Early Pleistocene *M.*  
610 *meridionalis* is characterized by low hypsodonty and a mean of 10–14 plates in the third molar,  
611 whereas *M. trogotherii* is both more hypsodont, with between 16 and 22 plates (Lister and Sher,  
612 2001). The published images of the Hama tooth allow confirmation of its identification as *M.*  
613 *meridionalis*, implying a greater age than the Latamneh fauna.

614 Consultation of SRTM imagery (Fig. 9) has confirmed that the deposits at Sharia ( $\leq 10$  m thick)  
615 are aggraded to ~40 m above the modern river, as originally suggested by Van Liere and Hooijer  
616 (1961), placing them within the height range of the sequence at Latamneh and making the  
617 attribution of both sites to QfIII seem entirely reasonable. Possible differences in uplift history

618 between the two localities cannot be ruled out however, which could explain the apparently older  
619 mammalian remains at Sharia. Indeed, Van Liere (1966) suggested that an older set of deposits,  
620 equivalent to those at Sharia, occurred at Latamneh and that the fossiliferous and handaxe-bearing  
621 sediments had subsequently been incised into them, although no later descriptions have confirmed a  
622 sequence of this sort.

623 The various biostratigraphical evidence thus requires the reattribution of the QfIII terrace, as  
624 represented at Latamneh and Sharia, to an age in the region of 1.2–0.9 Ma. This has a significant  
625 implication for the age model established for the Orontes by Bridgland et al. (2003; see above),  
626 which is confirmed as underestimated. Revised suggestions for the ages of terraces in the Hama–  
627 Latamneh area are indicated in Figure 7. The ~40 m height of the Sharia deposit suggests a  
628 significantly younger age than the aforementioned el-Farcheh site; the somewhat greater height of  
629 the deposits at Latamneh, notwithstanding the younger age, is attributed to a component of localized  
630 uplift in the vicinity of the adjacent Sheizar Fault (see below and Fig. 8A). Given this revision, it is  
631 no longer tenable to consider the Middle Orontes terraces as representative of formation in response  
632 to 100 ka Milankovitch climatic forcing (cf. Bridgland and Westaway, 2008a).

## 633 **6. The Ghab Basin**

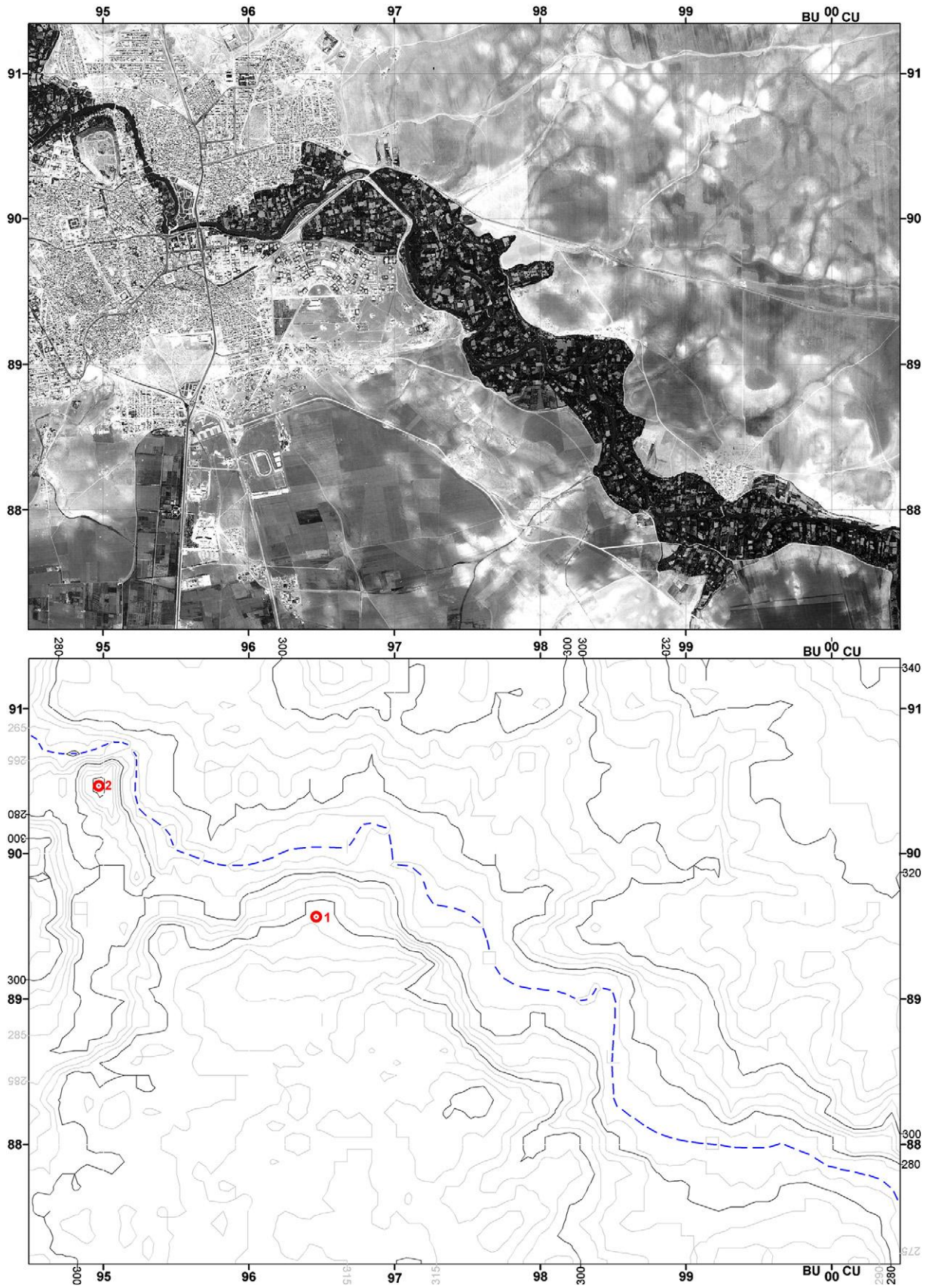
634 About 5 km downstream of Latamneh (along the valley axis) the Orontes leaves the incised part of  
635 its middle reach and enters the Acharneh Basin (located to the east of the southern part of the larger  
636 Ghab Basin: Fig. 1, inset), passing through a well-marked west-facing scarp slope close to the town  
637 of Sheizar (Fig. 8A). Further downstream the valley widens out within the Acharneh Basin to form  
638 a large flat plain and all but the lowest Pleistocene terraces disappear. These lowest terraces are  
639 represented on the maps of Besançon and Sanlaville (1993a, b) by widespread glacis, mostly  
640 forming apparent fans that extend westwards from the scarp; a few of the highest fragments of these  
641 are mapped as QfIII, although QfI and QfII dominate and extend along the course of the river  
642 downstream to Acharneh, beyond which they too cease to be represented (Fig. 10). Sections  
643 beneath the glacis surfaces in the latter area reveal them to be formed on lacustrine sediment of the  
644 Acharneh Basin (Devyatkin et al., 1997), probably Neogene in age, that have been slightly uplifted.  
645 Downstream of Acharneh the resumes its northward course, flowing above the stacked infill of the  
646 Ghab Basin (Fig. 3); this has been widely interpreted as an actively developing pull-apart basin  
647 (Devyatkin et al., 1997; Brew et al., 2001; Westaway, 2004b, 2010) the formation of which was  
648 probably broadly synchronous with the comparable Hula Basin further south, the initiation of the  
649 latter being reliably dated to ~4 Ma from its associated volcanism (Heimann and Steinitz, 1989;  
650 Heimann et al., 2009). These structures thus reflect the development of the present geometry of the

651 DSFZ, which came into being around that time, at ~3.7–3.6 Ma (Westaway et al., 2004b, 2010;  
652 Seyrek et al., 2007). The fact that fluvial aggradational terraces occur only upstream of the Sheizar  
653 scarp implies that the latter has formed in response to Pleistocene dip-slip (down-to-the-west)  
654 movement of a fault at this location (Figs 3 and 8A). This interpretation was suggested by de  
655 Heinzelin (1966) but was overlooked by later workers; indeed, de Heinzelin envisaged that the  
656 succession at Latamneh (see above) was deposited before this fault became active, at a time when  
657 much of the present relief of the area did not exist. Movement on this fault can be presumed to  
658 account for the lack of fluvial incision in the area downstream and the greater-than-expected height  
659 (give their biostratigraphical age) of the deposits at Latamneh, ~5 km upstream.

660 Much work was carried out in the Ghab by Russian scientists during the Soviet era, as reviewed by  
661 Domas (1994) and Devyatkin et al. (1997), who described a mixed lacustrine and fluvial Pliocene  
662 infill that, from geophysical evidence, attains a maximum thickness of 0.8–1.0 km. According to  
663 Devyatkin et al. (1997), the maximum sediment thickness occurs in the central–southern part of the  
664 basin, thinning to <200 m in the north (Fig. 1, inset). They also reported a lacustrine fill of up to  
665 ~300 m in the Acharneh Basin. A longitudinal section through the northernmost part of the Ghab,  
666 based on borehole evidence (Besançon and Sanlaville, 1993b), shows the majority of the infill,  
667 proved to a maximum thickness of 40 m (but unbottomed), to be Pliocene shelly clay, with  
668 interbedded sands, volcanic ash and, at the northern end of the basin, basaltic lava (Fig. 11B). This  
669 lava, erupted from poorly preserved cones to the north and east of the downstream limit of the  
670 Ghab, has been attributed to the Pliocene (Ponikarov et al., 1963b; Ponikarov, 1986; Domas, 1994),  
671 although it has yielded K–Ar dates as young as  $1.1 \pm 0.2$  and  $1.3 \pm 0.9$  Ma (e.g. Devyatkin et al., 1997).

672 It is unclear whether the Ghab has been continuously occupied by a lake throughout the Pleistocene  
673 or whether there were periods when the Orontes flowed across a dry lake floor, as at present  
674 (following anthropogenic drainage). As it approaches the northern end of the Ghab, the modern  
675 Orontes channel becomes increasingly deeply incised, partly, perhaps, as a result of the artificial  
676 drainage during the 1950s of what was, in historical times, a wetland (Besançon and Sanlaville,  
677 1993b). In part, however, this is likely to be a consequence of the river cutting into the basalt  
678 barrier as it passes from the subsiding basin interior into an area that has clearly been uplifting.  
679 There is evidence for uplift of the basalt barrier during the Quaternary, in the form of inset low-  
680 level river terrace gravels that border the course of the Orontes along the northernmost 15 km of the  
681 Ghab (Domas, 1994). These deposits are well exposed at Karkour, near the northern end of the  
682 basin, where Quaternary gravel was recorded by Van Liere (1961) and Besançon and Sanlaville

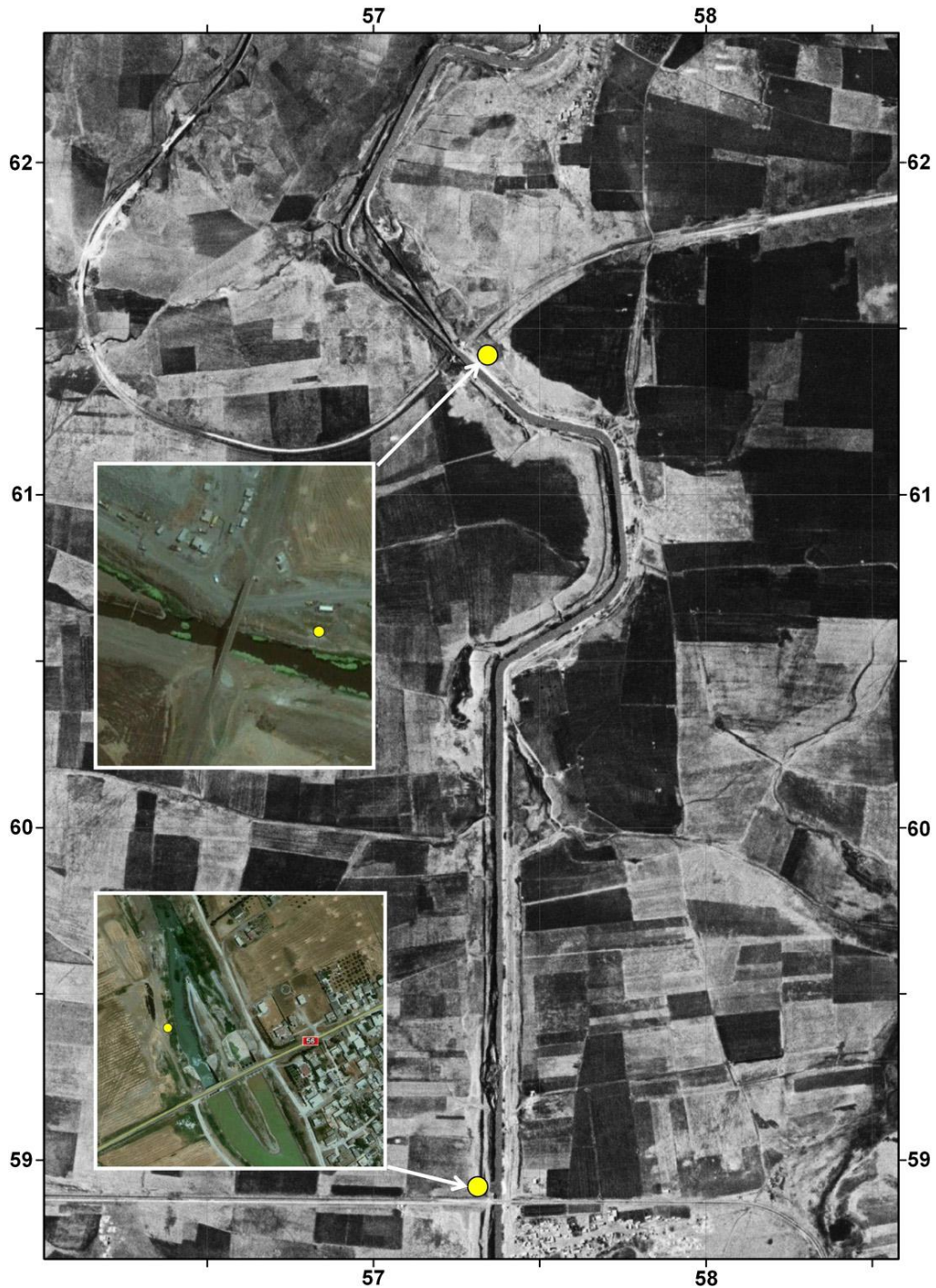
683 (1993b, their figure 19). Two gravel exposures were recorded during fieldwork in 2007, both in the



684

685  
686  
687  
688

**Fig. 9.** Paired images showing the *M. meridionalis* locality at Sharia, Hama: upper- GAMBIT image, taken in 1967; lower SRTM-derived contour image, with selected 5 m interval contours labelled and the Sharia locality indicated, centre left (as Point 1) in what was in 1967 the south-eastern edge of the Hama conurbation (UTM coordinates: BU 965 896). Point 2 is the ancient citadel in the centre of Hama. Coordinates are marked for 1 km grid squares.



689

690  
691  
692

**Fig. 10.** Fossiliferous sites in the Ghab Basin: 1960s CORONA image showing the location of (from north to south) the Karkour railway bridge and Karkour sluice sites at the northern end of the Ghab; note that the railway was under construction, with the bridge not yet in place. Insets show the location of sample points from present-day Google Earth. Coordinates are marked for 1 km grid squares, although the image shows a 0.5 km grid.

693

694

695

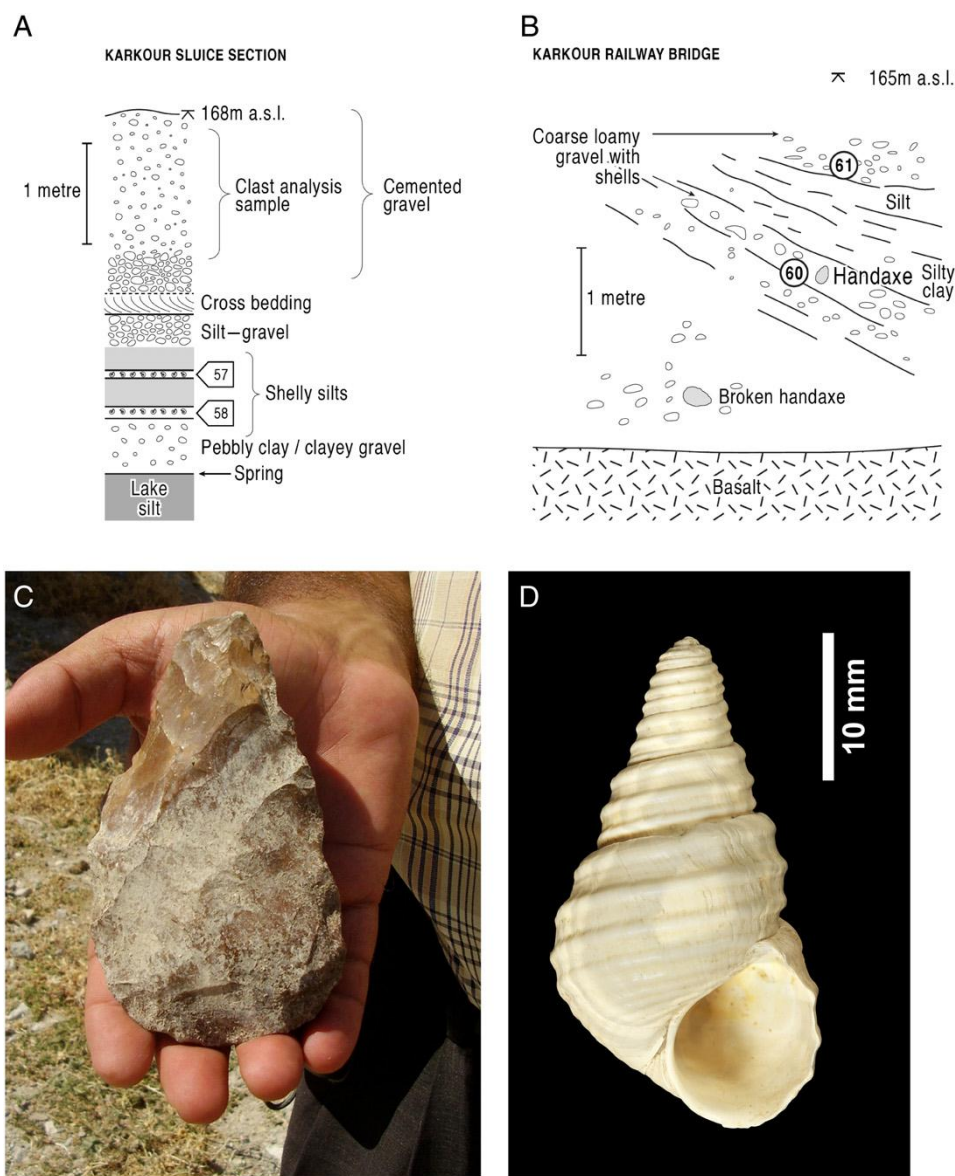
696

697

698

incised banks of the Orontes. First, at Karkour sluice (BV 57282 59073; ~168 m a.s.l.), 1–2 m of cemented medium–fine gravel was exposed, capping an unconsolidated sequence of shelly silts and fine sands above a lower clayey gravel–pebbly clay and culminating in fine gravel with an argillaceous matrix; the basal cemented gravel reveals cross bedding indicative of northward palaeoflow (Fig. 11A; online supplement, Fig. A.1.7). Analysis of the cemented gravel, carried out in the field (as in the Upper Orontes), showed that it comprises >95% flint/chert (Table 1), the only

699 other constituent being limestone, which has presumably been introduced from the sides of the  
 700 basin. Some 2.5 km further north, at the Karkour railway bridge (BV 57306 61493; 165 m a.s.l.), a  
 701 second gravel exposure was observed. The deposit here, which overlies the basalt that gives rise to  
 702 the knick point at the northern end of the Ghab, is much coarser than that further south, containing  
 703 large weathered basalt clasts. It is ~3 m thick, has a variable argillaceous matrix and contains  
 704 shells, including large gastropods (see below; online supplement, Fig. A.1.8). It also yielded a well-  
 705 preserved handaxe (Fig. 11B) and a butt fragment from a larger handaxe. The flint/chert reaching  
 706 Karkour has evidently been transported from the Middle Orontes upstream of Sheizar, avoiding  
 707 deposition as part of the thick stacked succession in the Ghab Basin. Analysis of samples from the  
 708 two Karkour sites has shown that the sediments contain ostracods as well as molluscs.



709

710 **Fig. 11.** Karkour, northern Ghab Basin: A- Section log from the Karkour sluice locality; B- Section log from the Karkour railway bridge locality; C-  
 711 hand axe from the Karkour railway bridge section; D- *Apameaus apameae* from the Karkour railway bridge section. This species is named after  
 712 Apameaea, a Roman site in the Ghab.

713 **6.1 Palaeontology of the Ghab sediments**

714 Mollusca were analysed from both Karkour exposures (Table 3). Samples 57 and 58, from silty  
 715 deposits beneath the cemented gravel at Karkour sluice, yielded assemblages dominated by  
 716 *Dreissena bourguignati* (~95% of the total). Samples 60 and 61, from Karkour railway bridge, also  
 717 yielded well preserved shells, the most distinctive being the large viviparid gastropod *Apameaus*  
 718 *apameae* (formerly *Viviparus apameae*; Fig. 11C; cf. Sivan et al., 2006). Previous authors have  
 719 described other fossiliferous exposures in this general area (cf. Schütt, 1988; Devyatkin et al., 1997;  
 720 see online Appendix 3).

721

722 **Table 3:** Molluscan faunas from exposures at Karkour (for locations, see Fig. 10; for details see text)  
 723

	Sample			
	57	58	60	61
<i>Theodoxus jordani</i> (Sowerby)	+	+	+	+
<i>Theodoxus orontis</i> Schütt				+
<i>Apameus apameae</i> (Blanckenhorn)			+	+
<i>Melanopsis blanckenhorni</i> Schütt	+	+	+	+
<i>Melanopsis uncinata</i> Blanckenhorn				+
<i>Melanopsis bicincta</i> Blanckenhorn				+
<i>Melanopsis cylindrata</i> Blanckenhorn				+
<i>Lymnaea</i> (? <i>Radix</i> ) sp.	+			
<i>Gyraulus piscinarium</i> Bourguignat			+	+
<i>Planorbis carinatus</i>				+
<i>Planorbis</i> sp.		+	+	+
<i>Valvata saulcyi</i> Bourguignat	+	+	+	+
<i>Semisalsa longiscata</i> (Bourguignat)	+	+		
<i>Bithynia applanata</i> Blanckenhorn	+	+		+
<i>Syrofontana fossilis</i> Schütt	+			+
<i>Falsipyrgula rabensis</i> (Blanckenhorn)	+	+		+
<i>Falsipyrgula ghabensis</i> Schütt	+	+		+
<i>Potomida kinzelbachi</i> Schütt			+	+
<i>Unio terminalis</i> Bourguignat			+	+
<i>Dreissena bourguignati</i> Locard	+	+	+	+

724

725

726 First described by Blanckenhorn (1897) based on shells from the Orontes, *A. apameae* is best known  
 727 from the Jordan valley, where it has been used as an index fossil to define the ‘upper freshwater  
 728 series’ or ‘*Viviparus* Beds’ of the Benot Ya’aqov Formation at Gesher Benot Ya’aqov (Picard,  
 729 1963; Tchernov, 1973; Goren-Inbar and Belizky, 1989; Bar-Yosef and Belmaker, 2010), noted  
 730 above as being somewhat more recent than the Latamneh deposits. As at Karkour, *A. apameae* is  
 731 found in direct association with handaxes at Gesher Benot Ya’aqov (Goren-Inbar and Belitzky,  
 732 1989; Goren-Inbar et al., 1992). The species became extinct in the Jordan Valley at ~240 ka, on the  
 733 basis of U-series dating (Kafri et al., 1983; Moshkovitz and Magaritz, 1987; Heller, 2007). Its first  
 734 appearance there followed the eruption of the Yarda Basalt, in the vicinity of the Sea of Galilee, and  
 735 of the Hazbani Basalt, which flowed from southern Lebanon into the Hula Basin in the

736 northernmost Jordan valley. Although dating of these basalt eruptions has been attempted using the  
 737 K–Ar method, this has not resulted in reliable age-determinations (e.g. Schattner and Weinberger,  
 738 2008). Given the data currently available, probably the best guide to the age of the Hazbani Basalt  
 739 and of the stacked succession in the Hula Basin is from the biostratigraphical and oxygen isotope  
 740 calibration by Moshkovitz and Magaritz (1987), based on borehole evidence. They recognized  
 741 glacial-to-interglacial termination IX (the MIS 20–19 transition) at a depth of ~160 m in the Hula  
 742 Basin fill, which implies that *A. apameae*, which occurred between depths of 67 and 168 m in the  
 743 studied borehole, had appeared by MIS 21. If it is assumed that the occurrence of this gastropod in  
 744 the Ghab was synchronous with its presence in the Jordan, then it can be concluded that the  
 745 sediments at Karkour railway bridge are Middle Pleistocene.

746

747 **Table 4:** Ostracod faunas from faunas from exposures at Karkour (for locations, see Fig. 10; for details see text)

	Sample	
	57	61
<i>Cyprideis torosa</i> (Jones)	+	+
<i>Ilyocypris</i> cf. <i>inermis</i> Kaufmann	+	
<i>Ilyocypris</i> sp. (spinose form)	+	+
<i>Loxoconcha</i> spp.	+	
<i>Candona neglecta</i> Sars	+	
<i>Candona</i> sp. (juveniles)		+
<i>Heterocypris salina</i> (Brady)		+
<i>Herpetocypris</i> sp.	+	

748

749 Samples 57 and 61 were also examined for ostracods, Sample 57 yielding the most abundant and  
 750 diverse fauna of seven species (Table 4), amongst which the most common was *Cyprideis torosa*.  
 751 The assemblages appear to include reworked and indigenous components, indicated by differential  
 752 preservation; the reworked material might be as old as Pliocene (see online Appendix 3). Pliocene–  
 753 Pleistocene ostracod faunas from the Levant region have been poorly documented, making this an  
 754 important record, particularly since these crustaceans are extremely valuable palaeolimnological  
 755 indicators (Holmes, 1996; Battarbee, 2000). For example, *C. torosa* occurs in brackish water,  
 756 developing noded valves in salinities below c. 5‰, but can also tolerate hypersaline conditions in  
 757 lakes and water bodies prone to desiccation. The indigenous component from the Karkour samples,  
 758 presumed to be Pleistocene, comprises both brackish (*C. torosa* and the loxoconchids) and  
 759 freshwater elements (*Candona neglecta*, *Ilyocypris* spp. and an unnamed *Heterocypris*).

760 The analysis of these two faunal groups thus supports a Pleistocene age for the sediments at both  
 761 Karkour sites, with reworked ostracods from earlier, possibly Pliocene sediments within the Ghab  
 762 Basin. It is worth highlighting the close similarities between the palaeontological and  
 763 archaeological material from the Ghab deposits at Karkour and the Benot Ya’aqov Formation in the

764 Jordan Valley; these records, coupled with the suggested contemporaneity of the Ghab and Hula  
765 basins, permits a tentative broad correlation to be suggested. This and the above-mentioned K–Ar  
766 dates for the basalt at the northern end of the Ghab implies an age range from the latest Early  
767 Pleistocene to Middle Pleistocene for the sedimentary succession at Karkour, rather than the  
768 Pliocene age previously suggested (cf. Ponikarov et al., 1963b), making it therefore somewhat  
769 younger than the deposits at Latamneh.

## 770 **7. The Orontes Gorge north of Jisr ash-Shugour**

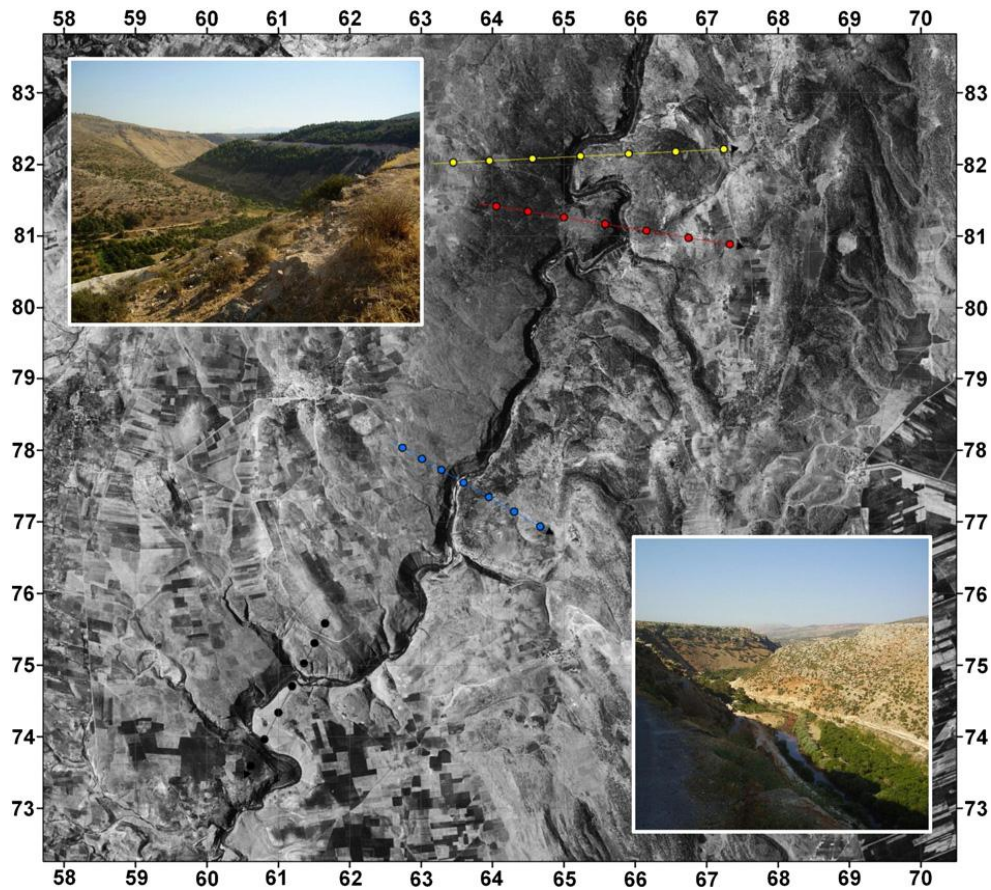
771 The town of Jisr ash-Shugour is situated at the downstream end of the Ghab Basin, north of which  
772 the Orontes enters a gorge, ~100 m deep (although within a wider, deeper feature up to 300 m deep)  
773 and ~25 km long (along its sinuosity; see Fig. 12; online supplement, Fig. A.1.9), that it has cut  
774 through Palaeogene limestone. At the northern end of the gorge is the town of Darkush, only 3 km  
775 upstream of the border with Hatay Province (Turkey).

776 Where this gorge could be accessed it was, unsurprisingly, found to contain no fluvial terraces, only  
777 a basal gravel ~0.3 m thick, beneath ~0.2 m of sand with gravel seams and capped by ~1.0 m of  
778 silty overbank deposits. This valley-floor sequence was observed and sampled at Hammam ash  
779 Sheykh Isa, where the gravel (126 m a.s.l.) proved to comprise mainly limestone (>99% of a  
780 somewhat undersized sample: Table 1). This demonstrates that the bedload of the Orontes has been  
781 recharged with limestone from the local Palaeogene outcrop, this having greatly diluted the  
782 flint/chert clasts that accounted for >95% of the gravel at Karkour.

783

## 784 **8. The Amik Basin, Hatay Province**

785 The meandering Orontes channel north-west of Darkush forms the border between Syria and Hatay  
786 for a (straight-line) distance of 23 km. To the north the river enters a second subsiding lacustrine  
787 basin, formerly occupied by Lake Amik. In this case the lake has disappeared during the last half  
788 century, having (along with its associated wetlands) occupied 53.3 km<sup>2</sup> in 1972 (Figs 1 and 13) but  
789 was eliminated completely by 1987 as a result of drainage for agriculture (Kiliç et al., 2006;  
790 Çalışkan, 2008; for notes on its earlier history, see Wilkinson, 1997; Yener et al., 2000). It was also  
791 known as the Lake of Antioch, the ancient city of that name (modern Antakya) being situated on the  
792 south-western extremity of the Amik Basin, the flat-topped infill of the latter giving rise to the  
793 Antioch/Amik Plain. The lake was drained by an artificial channel (the Balıkgölü Canal) into the  
794 Orontes, which flows along the southern edge of the basin without reaching the former site of the  
795 lake (Fig. 13).



796

797  
798  
799  
800  
801  
802  
803

**Fig. 12.** The gorge between Jisr ash-Shugour and Darkush: 1960s CORONA image of the gorge (for location, see Fig. 1); dotted lines show locations of derived cross sections (see online supplement, Fig. A.1.9). Coordinates are marked for 1 km grid squares. Insets show photographic images of the gorge: A- looking SSW (upstream) from BV 63205 76708, about 5 km east of Qanaya. The mountains visible in the far distance are part of the Jebel Nusayriyah range along the western side of the Ghab Basin.; B- Looking northwards, downstream along the valley, from BV 63234 76771. The gravel sample locality at Hammam ash Shaykh Isa is ~400 m to the north of the viewpoint, accessed from the nearer part of the valley-floor platform in the middle distance. Both photographs show features that might represent early river levels, although other explanations would be possible and ground-truthing has not been practicable.

804 Extending NNE (upstream) from the Amik Basin is the valley of the River Karasu, which follows  
 805 the alignment of the DSFZ as it trends in that direction, passing into the East Anatolian Fault Zone  
 806 (e.g. Westaway 2004b; Westaway et al., 2006; Fig. 1). The nature of faulting in this region was for  
 807 many years a subject of debate, in relation to controversy concerning the geometry of the DSFZ in  
 808 western Syria. Yurtmen et al. (2002) showed that the evidence was consistent with active faulting  
 809 along the Karasu valley continuing southward into the DSFZ, with no requirement for any other  
 810 large-scale faulting extending offshore to the south-west, as others had previously inferred. In this  
 811 view, the Amik Basin can be interpreted as marking a leftward step in the faulting, from the  
 812 Amanos Fault, which runs along the western margin of the Karasu valley, to the DSFZ segment  
 813 further south, which Westaway (2004b) called the Qanaya–Babatorun Fault. Subsequent analyses  
 814 (e.g. Seyrek et al., 2007, 2008; Westaway et al., 2008) have confirmed this general interpretation.  
 815 The Amik Basin can therefore be interpreted as another pull-apart basin within the DSFZ,  
 816 comparable with the Ghab. Although they have yet to be mapped in detail, the existence of active  
 817 faults in the region is corroborated by records of numerous large historical earthquakes (e.g. Akyuz

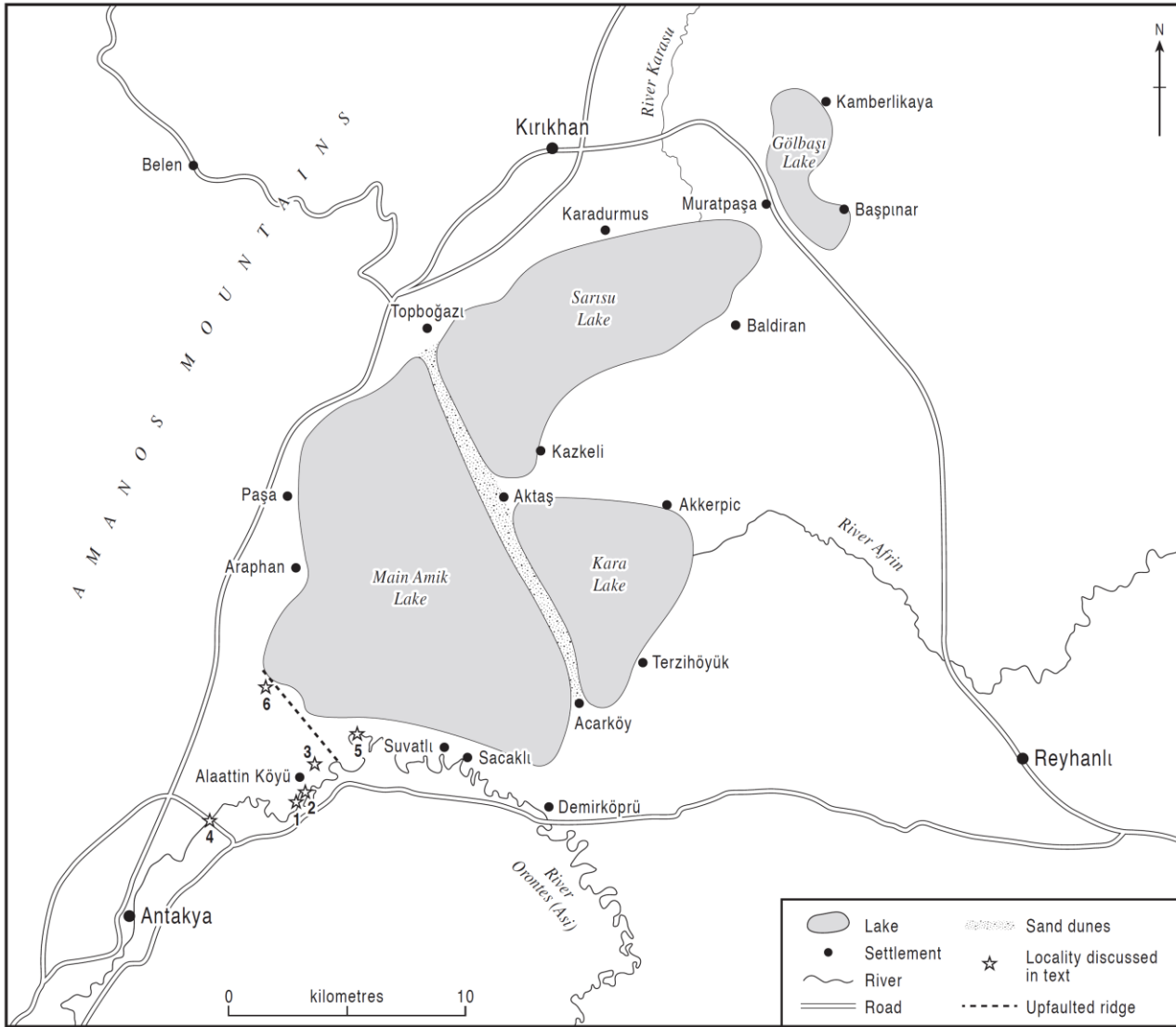
818 et al., 2006). The Karasu valley is the site of extensive eruptions of Quaternary basalt; offsets of  
819 dated basalt flows, where they cascade into the main valley along tributary gorges, have provided  
820 the principal method of measuring slip rates on faults in this region (e.g. Yurtmen et al., 2002;  
821 Seyrek et al., 2007).

822 It is difficult to study the Orontes to the south-east of the Amik Basin because of the political  
823 sensitivity of the Syria–Hatay border, with which it coincides in this area. Once downstream of the  
824 border, the river channel can readily be observed as it meanders extravagantly across the Amik  
825 Plain. Simple measurements at intervals demonstrate that the bed of the river becomes  
826 progressively incised below the surface of the plain as the outlet from the basin, near Antakya, is  
827 approached. The Orontes channel was measured as declining from ~3.5 m below the Antioch Plain  
828 at BA 54539 18533, ~2.5 km upstream of Alaattin, to ~9.5 m on the northern outskirts of Antakya  
829 (BA 48448 15139), over a (straight-line) distance of ~7 km (see Fig. 13, points 4 and 5).

830 Thin cobble-gravel, interbedded with floodplain silt, cropping out in the river bank (north side)  
831 ~2 m above the Orontes, ~1 km south of Alaattin Köyü (~86 m a.s.l.; Fig. 13, point 2; the source of  
832 a clast analysis sample: Table 1), was found to contain pottery, demonstrating a mid–late Holocene  
833 age, as well as freshwater mussel shells. Flint/chert from the Middle Orontes has increased in  
834 frequency in the river’s bedload here (~10%), in comparison with the Darkush Gorge sample  
835 locality ~50 km upstream, despite the much greater distance from its source outcrops than from the  
836 Palaeogene limestone (which has fallen to <75%: Table 1). This change can be attributed to the  
837 relative hardness and resistance to abrasion of the siliceous clasts, which persist into the gravels of  
838 the Lower Orontes, whereas the limestone disappears (see below; Table 1). The Amik Basin  
839 sample also contains a fresh input of crystalline material, notably local basalt (>10%), as well as  
840 coarser mafic rocks and traces of quartzitic, schistose and amphibolitic rocks. The coarse mafic  
841 rocks are likely to be from the latest Cretaceous Hatay ophiolite, whereas the other constituents are  
842 probably derived from the Precambrian/Palaeozoic succession exposed in the Amanos Mountains,  
843 west of the Karasu, by way of its right-bank tributaries. All such material is exotic to the Orontes  
844 valley upstream of this point.

845 Also exposed in the incised channel sides of the Orontes in the Amik Basin are horizontally  
846 laminated fine sands and silts, interpreted as fluvio-lacustrine sediments of Neogene–Quaternary  
847 age. They were observed in a river-bank section, ~1 km south of Alaattin (Fig. 13, point 1).  
848 Comparable deposits, although rather more indurated and gently tilted, were also observed in quarry  
849 sections in low hills standing above the Amik plain at Alaattin Köyü (Fig. 13, point 3). These  
850 would appear to represent upfaulted blocks of Neogene basin fill; at ~125 m a.s.l., the deposits have  
851 been uplifted ~40 m above the general level of the plain. The same upfaulted ridge reaches 159 m

852 a.s.l. to the north-west of Alaattin Köyü (Fig. 13, point 6). The absence of any other high ground  
 853 suggests that this area has been a subsiding sedimentary depocentre for most of recent geological  
 854 history and certainly since the present geometry of the DSFZ in this region came into being, in the  
 855 Mid Pliocene (~3.6–3.7 Ma; e.g. Seyrek et al., 2007; Westaway et al., 2008). A seismic reflection  
 856 profile published by Perinçek and Çemen (1990) indicates that the sedimentary fill in the Amik  
 857 Basin reaches a maximum thickness of ~1 km.



858

859 **Fig. 13.** The Amik basin showing the extent of the former Lake Amik (modified from Çalışkan, 2008). For location, see Fig. 1. Field localities are  
 860 numbered as follows (see text): 1, the Alaattin Köyü clast analysis locality (see Table 1); 2, river-bank section 1 km south of Alaattin Köyü (BA  
 861 52477 15506); 3, quarry section in upfaulted basin sediments at Alaattin Köyü (BA 52626 16772); 4 and 5, downstream and upstream limits of  
 862 measurement fluvial entrenchment beneath the Amik Plain (at BA 48448 15139 and BA 54539 18533, respectively); 6, spot-height in the upfaulted  
 863 sediment observed at 3, at 159 m a.s.l. (~BA 508 200).

864 **9. The Lower Orontes, downstream of Antakya**

865 Flowing south-westwards from Antakya, the Orontes again enters a high-relief area in which river  
 866 terrace deposits are preserved sporadically along its incised course (Erol, 1963), before entering the  
 867 most spectacular of its three gorges, more than 400 m deep, cut into resistant latest Cretaceous

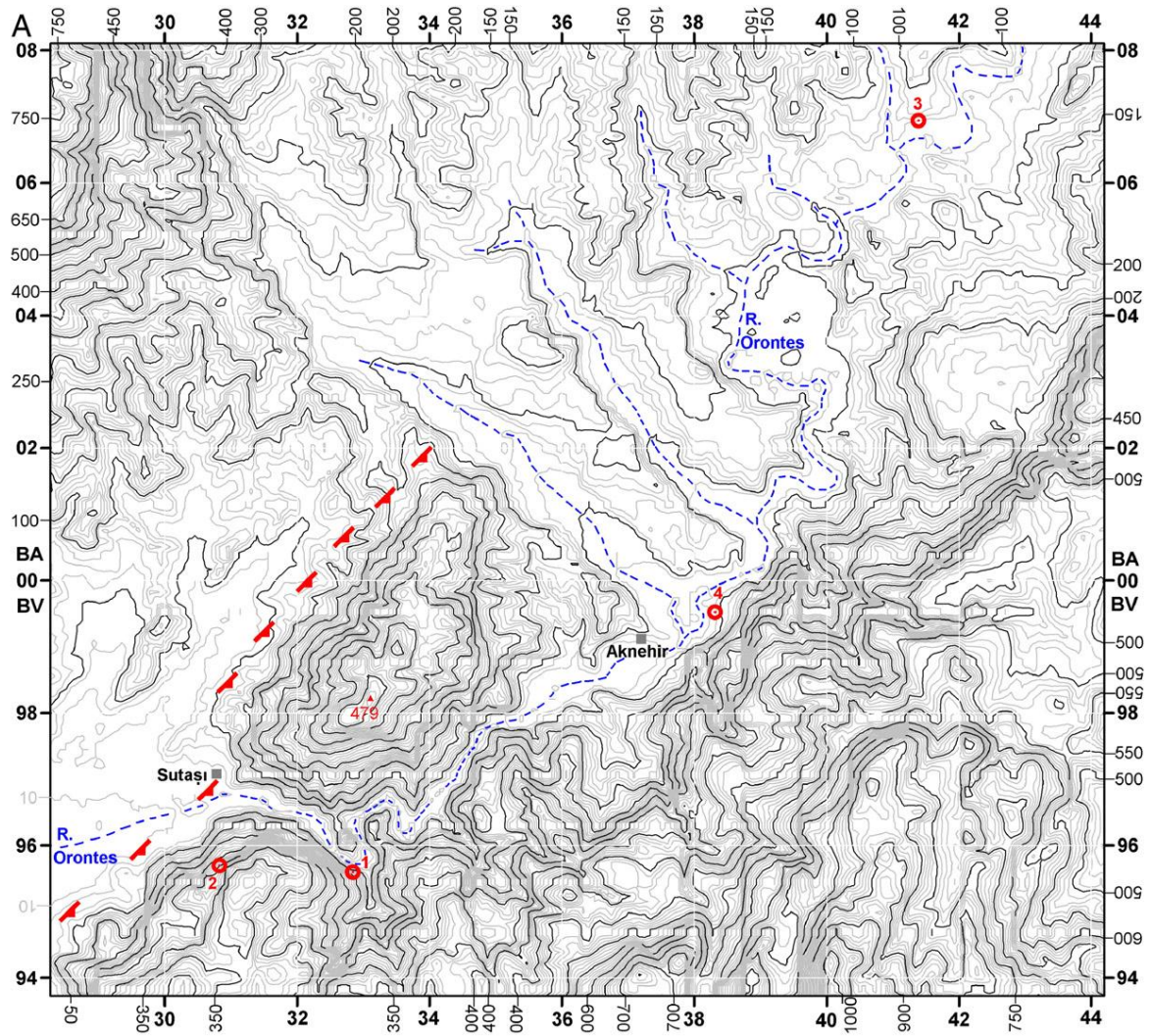
868 ophiolitic rocks (Figs 1 and 14). This incised valley makes a dramatic contrast with the low relief  
869 in the area of the Amik Plain. Between Aknehir and Sutaşı (BA 30927 97820), for a distance of ~8  
870 km, the Orontes follows a particularly deeply entrenched gorge between the Ziyaret Dağı mountain  
871 range to the southeast and the isolated Samandağ Tepe hill (summit 479 m a.s.l.) to the northwest.  
872 The abruptness of its downstream end (Fig. 14), where the Orontes flows out of a major escarpment  
873 that was recognized by Erol (1963), raises the possibility that it is caused by localized slip on an  
874 active dip-slip fault (Figs 3 and 14). A fault in this location, near the village of Sutaşı, was indeed  
875 indicated by Tolun and Erentöz (1962). Recent interpretations of the regional kinematics (e.g.  
876 Westaway, 2004b; Gomez et al., 2006; Seyrek et al., 2008; Abou Romieh et al., 2009) require a  
877 component of crustal shortening in the crustal blocks alongside the active left-lateral faults forming  
878 the northern DSFZ. It is thus probable that any dip-slip fault in the Antakya area, away from the  
879 main left-lateral faulting, would be a reverse fault (cf. Fig. 3) rather than a normal fault. Heights  
880 and tentative ages for the marine terraces on the Mediterranean coastline were reported by Erol  
881 (1963) and were used by Seyrek et al. (2008) to infer a typical uplift rate of  $\sim 0.2 \text{ mm a}^{-1}$  during the  
882 latter part of the Middle Pleistocene and the Late Pleistocene. The rate of localized uplift in the  
883 supposedly fault-bounded gorge reach may well be significantly higher than this already-high  
884 estimate of the regional uplift rate (cf. Demir et al., this issue).

885 In this gorge reach the Orontes falls 50 m in 16 km to the sea south of Samandağı. Former dock-  
886 side masonry of ancient Seleucia Pieria (the former port of Antioch) can be observed today within  
887 agricultural land (at YF 63841 00704), demonstrating relative sea-level fall in this area in the past  
888 two millennia. Relative sea-level decline has also been documented from the levels on the quayside  
889 masonry of borings by marine molluscs, at up to 0.75 m above modern sea level, and has been  
890 linked to historical earthquakes, notably one in AD 551 (Pirazzoli et al., 1991).

891 Study of gravel exposures in this Lower Orontes reach reveals a further input of the crystalline  
892 rocks first seen in the Amik Basin sample. For example, a sample collected near Bostancık Köyü  
893 (Fig. 14), from an Orontes terrace gravel exposed on the western side of the Antakya western  
894 bypass (76 m a.s.l.;  $\sim 25$  m above the river), contained  $\sim 30\%$  basalt and  $>50\%$  coarser basaltic  
895 lithologies, both including badly weathered examples (Table 1). Highly weathered ophiolitic rocks  
896 were also encountered (14.4%), as well as quartzose lithologies and kaolinized rocks (Table 1).

897 Only a single flint/chert clast was recorded in this sample, which was devoid of limestone. In  
898 contrast, a sample collected from a bluff on the left bank of the Orontes at Şahin Tepesi,  $\sim 25$  m  
899 above the river (probably representing the same terrace, therefore), yielded 1.7% flint/chert and 7%

limestone, the latter assumed to be locally derived (from the Cretaceous marine succession onto



902 Fig. 14. A- Synthetic contour map generated from SRTM data showing the Orontes valley downstream of Antakya (for location, see Fig. 1). Faint  
 903 contours are at 10 m intervals, with dark contours at 50 m intervals, the latter omitted where the relief is too steep. Note the contrast between the broad valley upstream of Aknehir and the gorge reach between there and Sutaşı. The Sutaşı fault is marked, with ticks on the hanging wall. The  
 904 summit of Samandağ Tepe is marked by its ~479 m spot height. Numbered localities denote the following: 1, viewpoint for Fig. 14B; 2, viewpoint  
 905 for Fig. 14C; 3, Bostancık Köyü (Antakya western bypass) clast analysis locality; 4, the Şahin Tepesi clast analysis locality. B- Looking north-west  
 906 (downstream) from BV 32785 95604 along the entrenched gorge reach shown in A. C- Looking NNE from BV 30827 95697 across the exit of the  
 907 Orontes gorge at the village of Sutaşı, where the river emerges from what is interpreted as a locally uplifted fault block, the margin of which also  
 908 creates the abrupt escarpment below the viewpoint.  
 909

910 which the Hatay ophiolite has been emplaced; e.g. Tolun and Erentöz, 1962) rather than transported  
911 from Syria. It was comparable with the previous sample in that it was dominated by basalt and  
912 coarser basaltic rocks, together with ophiolite and a trace of quartzitic lithologies (Table 1). Erol  
913 (1963) included the terrace deposits here as part of his Orontes Terrace II, which is the lowest of the  
914 terraces depicted in Figure 3 (his lowest terrace being too close to the river to show at this scale).  
915 He correlated this fluvial terrace with his Marine Terrace II, which Seyrek et al. (2008) concluded  
916 to be of last interglacial (MIS 5e) age. A direct correlation between fluvial and marine terraces, and  
917 Erol's (1963) resulting age assignment of this fluvial terrace to the 'Riss–Würm Interglacial', is  
918 unlikely to be tenable, given that current wisdom generally attributes river terrace gravels to cold-  
919 climate episodes (e.g. Bridgland, 2000; Bridgland and Westaway, 2008b; Bridgland et al., 2008).  
920 The reported heights of Erol's (1963) five Orontes terraces in the reach between Bostancık Köyü  
921 and the upstream end of the Samandağ Tepe gorge, 5–7, 15–25, 40–50, 70–80, and 90–100 m above  
922 the modern river, are indicative of a regular pattern, suggesting terrace formation in response to 100  
923 ka climatic cycles, as in other parts of the world (cf. Bridgland, 2000; Bridgland and Westaway,  
924 2008a). The reported terraces can perhaps be correlated with MIS 12, 10, 8, 6 and 2. Uplift rates in  
925 this reach of the river during this span of time would thus approach  $0.2 \text{ mm a}^{-1}$ , far higher than in  
926 localities further upstream. Like in the Ceyhan valley through the Amanos Mountains further north  
927 (Seyrek et al., 2008), and in the lower reaches of the Nahr el-Kebir near Latakia in NW Syria  
928 (Bridgland et al., 2008), the absence of any earlier record in this reach of the Orontes can be  
929 attributed to the rapid uplift; the resulting high relief and the associated rates of slope processes  
930 have led to low probabilities for preservation of older river terrace deposits.

## 931 **10. Discussion: possible age and relation to climatic fluctuation**

932 Unlike other nearby rivers in Turkey and Syria (Sharkov et al., 1998; Bridgland et al., 2007; Demir  
933 et al., 2007, this issue; Seyrek et al., 2008; Westaway et al., 2009b), there are no Pleistocene lava  
934 flows interbedded within the Pleistocene terrace sequence of the Orontes to provide marker levels  
935 for dating, although the Homs Basalt provides a maximum age for the start of incision by the upper  
936 river below the level of the Late Miocene–Early Pliocene lake bed onto which this lava erupted. It  
937 has been thought, therefore, that the best indication of age within the sequence comes from the  
938 mammalian assemblage from the Middle Orontes (see above). Indeed, Bridgland et al. (2003)  
939 previously used the Latamneh terrace deposits as a pinning point for correlation between the Middle  
940 and Upper Orontes terrace sequences, having also modelled the latter (see also Bridgland and  
941 Westaway, 2008a) using the technique applied widely to terrace systems elsewhere (Westaway,  
942 2004a; Westaway et al., 2002; see above). They attributed the formation of comparable terrace  
943 sequences in both the middle and upper reaches of the Orontes to cyclic climatic forcing of fluvial

944 sedimentation and erosion with progressive incision in response to regional uplift. The similarity of  
945 these records to those in rivers elsewhere, notwithstanding proximity to plate boundaries (as in the  
946 case of the Orontes) or otherwise (as in rivers in NW Europe with similar uplift histories) was also  
947 noted (Bridgland et al., 2003; Bridgland and Westaway, 2008a). The consistent pattern of uplift,  
948 seen widely and calibrated in systems with optimal dating control, records acceleration at around 3  
949 Ma, followed in many cases by renewed acceleration around 2 Ma, then by decrease during the  
950 Early Pleistocene and a further acceleration at around the ‘Mid-Pleistocene Revolution’, when the  
951 100 ka climate cycles began (Bridgland and Westaway, 2008b; Westaway et al., 2009a). Each of  
952 these phases of uplift is well developed in fluvial sequences within the Arabian Platform, notably  
953 that of the River Euphrates (e.g. Demir et al., 2007, 2008; Westaway, 2010). This pattern of  
954 persistent uplift is seen, however, only in areas of post-Early Proterozoic (i.e. non-cratonic) crust,  
955 older crust being colder and more stable and showing either intermittent uplift and subsidence  
956 (Early Proterozoic crust) or, in the case of Archaean cratons, little vertical movement at all during  
957 the Late Cenozoic (Westaway et al., 2003, 2009a; Westaway, this issue). Subsiding areas of  
958 sediment accumulation are further exceptions to the standard pattern; not necessarily fault bounded,  
959 their subsidence is presumed to be a response to sedimentary isostasy. Examples of substantial  
960 subsiding regions of this type are the Lower Rhine, beneath the Netherlands (Brunnacker et al.,  
961 1982; Ruegg, 1994), and the Great Hungarian Plain (Gábris and Nádor, 2007; Kasse et al., 2010).  
962 Smaller areas of subsidence are also recognized within the Rhine, such as the Neuwied Basin,  
963 where a substantial stacked sequence of fluvial deposits floors a down-faulted block (Meyer and  
964 Stets, 2002). The Ghab and Amik Basins compare closely with the last-mentioned European  
965 example, as they also occupy small subsiding fault-bounded blocks.

966 It is apparent from the disposition of fluvial gravel terraces in both the Upper and Middle Orontes  
967 that the river in both these reaches has migrated westwards during the Pleistocene, although  
968 throughout that time it flowed between them through the fixed and entrenched Rastan Gorge. The  
969 close coincidence of the modern Orontes course and the eastern margin of the Homs Basalt outcrop  
970 can be explained as the result of this westward migration being prevented once the river  
971 encountered the resistant basalt, with forms an eastward-inclined interbed within the ‘Pontian’  
972 lacustrine marl.

973 The previous use of the Latamneh deposits as a dating level within the Orontes sequence must now  
974 be open to question, since, as noted above, the mammalian assemblage from that locality includes  
975 elements that date back to the late Early Pleistocene and would seem to imply an age in the region  
976 of 1.2–0.9 Ma. This revision (Fig. 7) effectively doubles the supposed age of the QfIII terrace at  
977 Latamneh, with the clear implication that uplift there has been at half the rate previously supposed.

978 Account must also be taken of the contradictory indications from the occurrences of different  
979 mammoth species within deposits mapped as Terrace QfIII at Latamneh (*M. trogontherii*) and  
980 Sharia, Hama (*M. meridionalis*), the latter being potentially an older indicator than even the  
981 arvicolid *L. arankae* at Latamneh. It is also now evident that the Latamneh locality is within a few  
982 kilometres of an active fault, at Sheizar, that has experienced significant movement during the  
983 Pleistocene. It is thus possible that the deposits there might provide a less-than-reliable indication  
984 of the regional uplift rate in the Middle Orontes valley, which could explain the indication that older  
985 deposits occur at a lower height relative to the modern river in the Hama area. The deposits in the  
986 latter area are ~30 km upstream of the faulting and can be assumed to provide a genuine indication  
987 of the regional uplift. It is nonetheless clear that the deposits of Middle Orontes Terrace QfIII are  
988 significantly older than was suggested in previous publications (cf. Sanlaville, 1988; Bridgland et  
989 al., 2003).

990

991 The reinterpretation of the Middle Orontes record raises the possibility that it is comparable with  
992 that from other parts of the Arabian Platform, further east in Syria and to the north-east in Turkey,  
993 where it has been discerned from the terrace sequence of the River Euphrates. Evidence from the  
994 Euphrates points to relatively slow uplift and to a brief period of subsidence in the late Early  
995 Pleistocene, during which the valley was partly backfilled with fluvial sediment (Demir et al., 2007,  
996 2008, this issue). The resultant thick aggradation, culminating at about MIS 22, has yielded  
997 numerous handaxes, although the Euphrates sediments are generally devoid of fossils. It is  
998 tempting, therefore, to suggest a correlation with the deposits at Latamneh, which also indicate  
999 thick sediment accumulation, have an age (from biostratigraphy) close to the Early–Middle  
1000 Pleistocene boundary and contain numerous handaxes. The comparable localities in the Euphrates,  
1001 indicative of subsidence in the late Early Pleistocene, include sites such as Ain Abu Jemaa, near  
1002 Deir ez-Zor, Syria (Demir et al., 2007), and Birecik and Karababa, in southeastern Turkey (Demir et  
1003 al., 2008, this issue). A physical mechanism for the reversals in vertical crustal motion that are  
1004 implicit in this interpretation is suggested by Westaway (this issue). The subsequent increase in  
1005 regional uplift rates that caused a switch from aggradation back to incision in these rivers can be  
1006 attributed to the Mid-Pleistocene Revolution, with the more severe cold stages that occurred within  
1007 the subsequent 100 ka climate cycles leading to enhanced climatic forcing and a positive-feedback  
1008 enhancement of erosional isostasy. At Latamneh area this effect might well have been accentuated  
1009 by the component of vertical slip on the Sheizar Fault (cf. de Heinzelin, 1966). Indeed, it is  
1010 conceivable that increased rates of vertical motion in opposite senses (i.e. faster uplift in the Middle  
1011 Orontes and faster subsidence in the southern Ghab Basin) following the Mid-Pleistocene

1012 Revolution affected the state of stress in the region, resulting in initiation or reactivation of slip on  
1013 the Sheizar Fault (cf. Westaway, 2006).

1014

1015 There is scant evidence that late Early Pleistocene subsidence occurred further upstream in the  
1016 Orontes. Recalibration of the ages of the Upper Orontes terraces (cf. Fig. 4) generally suggests that  
1017 the Bridgland et al. (2003) age model underestimates their ages by a single Milankovitch (100 ka)  
1018 cycle, given that the number and spacing of the terraces remains suggestive of formation in  
1019 approximate synchrony with these glacial–interglacial cycles. The more rapid uplift, in comparison  
1020 with the Middle Orontes, that is implicit in this interpretation is in keeping with the evident post-  
1021 Pliocene uplift of the ‘Pontian’ lacustrine basin (cf. Fig. 3).

1022

1023 The dating river gorges is, in general, difficult and typically relies upon projection of terraces from  
1024 upstream and downstream (cf. Fig. 3). The Rastan Gorge is, in fact, an exception, since its incision  
1025 can also be constrained by the ages of the Homs and Tell Bisseh Basalt. In particular, the well-  
1026 constrained age of the Homs basalt provides an upper limit on the ages of the oldest terraces,  
1027 comparable in height above the river (Fig. 3), of ~4–5 Ma . It is much more difficult to be clear  
1028 about the age of the Darkush Gorge, since it is isolated from well-dated terrace sequences, falling  
1029 between the subsiding Ghab and Amik basins.

1030 In contrast to the Upper and Middle Orontes catchment, much higher rates of vertical crustal motion  
1031 are indicated in coastal parts of the study region. Setting aside any local effects of active faulting,  
1032 as already noted, the disposition of the Orontes and marine terraces downstream of Antakya  
1033 indicates an uplift rate of ~0.2 mm a<sup>-1</sup>, roughly an order-of-magnitude faster than estimates for the  
1034 Middle Orontes, where the inferred ~120 m of incision in the Hama reach since ~4 Ma (Early  
1035 Pliocene) equates to a rate of ~0.03 mm a<sup>-1</sup>, although if the deposit at Sharia, ~40 m above the  
1036 modern river, is as young as ~1 Ma it indicates an accelerated rate of ~0.04 mm a<sup>-1</sup> during the last  
1037 million years. This estimate of the regional uplift rate can be compared with an independent  
1038 estimate of ~0.4 mm a<sup>-1</sup> further north in the Amanos mountain range, based on the terraces of the  
1039 River Ceyhan, which are capped by datable basalt flows (Seyrek et al., 2008). The uplift rate is also  
1040 ~0.4 mm a<sup>-1</sup> further south in the Latakia area of north-west Syria, on the basis of marine and fluvial  
1041 terraces in the region of the Nahr el-Kebir estuary (Bridgland et al., 2008), the latter river draining a  
1042 catchment that lies entirely seaward from the course of the Orontes (Fig. 1, inset). Seyrek et al.  
1043 (2008) reported on a modelling study that attempted to establish the cause of the high uplift rates in  
1044 these coastal regions, which lie close enough to the DSFZ for it to be possible that they are affected  
1045 by the distributed crustal shortening (as well as localized faulting) that is required given the

1046 orientation and slip sense of this fault zone. However, they found that this process is unlikely to be  
1047 the main cause of the rapid regional uplift observed, concluding instead that this is primarily the  
1048 isostatic response to erosion. They envisaged a complex sequence of events, with positive feedback  
1049 effects, following the elevation of the coastal mountain ranges as a result of plate motions (once the  
1050 modern geometry of the plate boundary zone was established at ~4 Ma). Once some initial  
1051 topography had developed, orographic precipitation would have been initiated in this coastal region,  
1052 as a result of westerly winds from the Mediterranean. The resulting rainfall in turn triggered  
1053 erosion, and, given the physical properties of the underlying crust (cf. Bridgland and Westaway,  
1054 2008a, b), the resultant unloading drove the observed uplift isostatically. Conversely, sediment  
1055 loads, triggered by the same combination of processes, may well have driven the observed  
1056 subsidence in depocentres such as the Ghab and Amik basins. It thus appears likely that both plate  
1057 motions and climate have contributed to the pattern of vertical crustal motions in this coastal region,  
1058 whereas parts of the arid interior hinterland that are well away from any active faults, such as the  
1059 Hama area, have experienced much slower uplift, reflecting the lower rates of erosion.

1060 The difference between the  $\sim 0.2 \text{ mm a}^{-1}$  uplift estimated for the lower Orontes downstream of  
1061 Antakya and the  $\sim 0.4 \text{ mm a}^{-1}$  rates in the other coastal regions may result from a significant part of  
1062 the deformation in the former area being accommodated by local reverse faults, such as that at  
1063 Sutaşı (see above; Figs 3 and 14), whereas in the regions traversed by the Ceyhan and Nahr el-Kebir  
1064 it is accommodated entirely by distributed crustal deformation. It is thus possible that the spatial  
1065 average of the uplift rates in the terraced reach of the Lower Orontes downstream of Antakya and in  
1066 the gorge reach in the hanging wall of the Sutaşı Fault equate to  $\sim 0.4 \text{ mm a}^{-1}$ . However, there is no  
1067 way of estimating directly the local uplift rate in this gorge reach to facilitate such a comparison.

1068 In the Upper Orontes the uplift rate appears to be significantly higher than in the Middle Orontes;  
1069 the age model in Fig. 4 indicates a time-averaged rate since the Mid-Pleistocene Revolution of  
1070  $\sim 0.09 \text{ mm a}^{-1}$ , more than double the upper bound of  $\sim 0.04 \text{ mm a}^{-1}$  for the Middle Orontes over a  
1071 similar interval, based on the supposed age of the Sharia deposits (see above). This difference may  
1072 possibly reflect the relative erodability of the 'Pontian' marl substrate in the Homs area (i.e., faster  
1073 erosion is resulting in a faster isostatic uplift response). Alternatively, much of the study region  
1074 south of Homs adjoins the NNE end of the Anti-Lebanon mountain range and the western end of  
1075 the Palmyra Fold Belt (Fig. 1). It is thus possible that localities in this region are affected by  
1076 components of localized deformation (possibly arising from slip on blind reverse faults beneath  
1077 anticlines; cf. Demir et al., this issue). Abou Romieh et al. (2009) indeed noted localized  
1078 deformation of Euphrates terraces where the Palmyra Fold Belt crosses this river valley in NE

1079 Syria, and inferred significant rates of deformation in more westerly parts of this deforming zone.  
1080 Demir et al. (this issue) have shown that the heights of Euphrates terraces in SE Turkey vary  
1081 laterally because rates of localized deformation on active faults and folds can be significant  
1082 compared with regional uplift rates.

## 1083 **11. Conclusions**

1084 The work on the Orontes, reported here, testifies to the value of a pragmatic approach, using  
1085 multiple techniques and taking account of data from all relevant sources, in this case field and GIS  
1086 survey of terrace morphology and sediments (assisted by dGPS), the use of fossil and artefact  
1087 content as indicators of age for particular terrace formations, of clast analysis to identify the  
1088 deposits of this river (as opposed to tributaries) and mathematical modelling, to provide a broad  
1089 impression of likely ages, calibrated by pinning points and other constraints.

1090

1091 The variable Quaternary record from different reaches of the Orontes underlines the role in crustal  
1092 properties and of climate in controlling landscape evolution within particular regions. Although  
1093 less well dated than sequences in nearby catchments in Syria and Turkey, it is possible, using the  
1094 starting point of the Homs Basalt eruption and the limited biostratigraphical and geochronological  
1095 constraint (the last from the U-series dating reported here for the first time), to erect tentative age  
1096 models for the sequences in the key reaches. This can be compared with those applicable to  
1097 neighbouring catchments, in particular the slowly uplifting interior of the Arabian Platform  
1098 (transacted by the Euphrates), to which the Middle Orontes can be likened, and the rapidly uplifting  
1099 coastal area that extends both north and south of, as well as including, the lowermost Orontes (cf.  
1100 Fig. 3). The repeated changes along the course of the river between uplifting crustal blocks (with  
1101 either terraces or gorges, according to the relative resistance of the bedrock) and subsiding ones is  
1102 the major contribution of active Quaternary crustal deformation; otherwise the disposition of  
1103 terraces in those reaches where they have formed is comparable with regions of post-Archaeon crust  
1104 elsewhere in the world (Bridgland and Westaway, 2008a, b; Westaway et al., 2009a). The  
1105 contrasting record from the different reaches of this single river thus provides valuable insight into  
1106 the contrasting types of records from rivers elsewhere that are wholly within individual crustal  
1107 blocks.

1108

## 1109 **Acknowledgements**

1110 This research includes work that was part of the project ‘Settlement and Landscape Development in  
1111 the Homs Region, Syria’, a joint project of the University of Durham and the Directorate General of

1112 Antiquities and Museums (DGAM), Syria, and funded by the Council for British Research in the  
1113 Levant (CBRL). We wish to thank the ‘Fragile Crescent Project’ (funded by the Arts and  
1114 Humanities Research Council, UK) for providing us with satellite imagery data. The research also  
1115 includes work undertaken using CBRL funding awarded to DRB, latterly supported through  
1116 collaboration with the National Earthquake Center, Damascus, which has supplied both scientific  
1117 expertise and logistical assistance. Work in Turkey has been funded in part by HÜBAK, the  
1118 research fund of Harran University (grants to TD and AS).

## 1119 **References**

1120 Abou Romieh, M., Westaway, R., Daoud, M., Radwan Y., Yassminh, R., Khalil, A., al-Ashkar, A.,  
1121 Loughlin, S., Arrell, K., Bridgland, D., 2009. Active crustal shortening in NE Syria revealed by  
1122 deformed terraces of the River Euphrates. *Terra Nova* 27, 427–437.

1123 Akyuz, H.S., Altunel, E., Karabacak, V., Yalçiner, C.C., 2006. Historical earthquake activity of the  
1124 northern part of the Dead Sea Fault Zone, southern Turkey. *Tectonophysics* 426, 281–293.

1125 Bar-Yosef, O., Belmaker, M., 2010. Early and Middle Pleistocene Faunal and hominins dispersals  
1126 through Southwestern Asia, *Quaternary Science Reviews* 30, 1318–1337.

1127 Bartl, K., al-Maqdissi, M., 2005. Achäologische Oberflächenuntersuchungen im Gebiet zwischen ar-  
1128 Rastan und Qal'at Sayzar. In: *Orte und Zeiten, 25 Jahre archäologische Forschung in Syrien, 1980–*  
1129 *2005*, pp. 136–141. Damascus: Deutsches Archäologische Institut, Orient-Abteilung, Außenstelle  
1130 Damaskus.

1131 Battarbee, R.W., 2000. Palaeolimnological approaches to climate change, with special regard to the  
1132 biological record. *Quaternary Science Reviews* 19, 107–124.

1133 Besançon, J., Sanlaville, P., 1993a. La vallée de l'Oronte entre Rastane et Aacharné. In: Sanlaville,  
1134 P., Besançon, J., Copeland, L., Muhesen, S. (Eds.), *Le Paléolithique de la vallée moyenne de*  
1135 *l'Oronte (Syrie): Peuplement et environnement*. *British Archaeological Review, International*  
1136 *Series*, vol. 587, pp. 13–39.

1137

1138 Besançon, J., Sanlaville, P., 1993b. Remarques sur la géomorphologie du Ghab (Syrie). In:  
1139 Sanlaville, P., Besançon, J., Copeland, L., Muhesen, S. (Eds.), *Le Paléolithique de la vallée*

- 1140 moyenne de l'Oronte (Syrie): Peuplement et environnement. *British Archaeological Review*,  
1141 *International Series*, vol. 587, pp. 41–54.
- 1142 Besançon, J., Copeland, L., Hours, F., Sanlaville, P., 1978a. The Palaeolithic sequence in  
1143 Quaternary formations of the Orontes river valley, northern Syria: a preliminary report. *Bulletin of*  
1144 *the Institute of Archaeology*, London 15, 149–170.
- 1145 Besançon, J., Copeland, L., Hours, F., Sanlaville, P., 1978b. Morphologie et préhistoire de la vallée  
1146 de l'Oronte entre Rastane et le Ghab. *Comptes Rendus de l'Académie des Sciences de Paris* 287,  
1147 857–860.
- 1148 Blankenhorn, M.L.P., 1897. Zur Kenntnis des Süßwasser Ablagerungen und Mollusken Syriens.  
1149 *Palaeontographica* 44, 1–144.
- 1150
- 1151 Brew, G., Lupa, J., Barazangi, M., Sawaf, T., Al-Imam, A., Zaza, T., 2001. Structure and tectonic  
1152 development of the Ghab basin and the Dead Sea fault system, Syria. *Journal of the Geological*  
1153 *Society of London* 158, 665–674.
- 1154
- 1155 Bridgland, D.R., 1986. *Clast lithological analysis. Technical Guide 3, Quaternary Research*  
1156 *Association*, Cambridge, 207 pp.
- 1157 Bridgland, D.R., 2000. River terrace systems in north-west Europe: an archive of environmental  
1158 change, uplift and early human occupation. *Quaternary Science Reviews* 19, 1293–1303.
- 1159 Bridgland, D.R., Westaway, R., 2008a. Climatically controlled river terrace staircases: a worldwide  
1160 Quaternary phenomenon. *Geomorphology* 98, 285–315.
- 1161 Bridgland, D.R., Westaway, R., 2008b. Preservation patterns of Late Cenozoic fluvial deposits and  
1162 their implications: results from IGCP 449. *Quaternary International* 189, 5–38.
- 1163 Bridgland, D.R., Demir, T., Seyrek, A., Pringle, M., Westaway, R., Beck, A.R., Rowbotham, G.,  
1164 Yurtmen, S., 2007. Dating Quaternary volcanism and incision by the River Tigris at Diyarbakır, SE  
1165 Turkey. *Journal of Quaternary Science* 22, 387–393.
- 1166 Bridgland, D.R., Philip, G., Westaway, R., White, M., 2003. A long Quaternary terrace sequence in  
1167 the Orontes River valley, Syria: a record of uplift and of human occupation. *Current Science (New*  
1168 *Delhi)* 84, 1080–1089.

- 1169 Bridgland, D.R., Westaway, R., Daoud, M., Yassminh, R., Abou Romieh, M., 2008. River Terraces  
1170 of the Nahr el Kebir, NW Syria, and their Palaeolithic record. *CBRL Bulletin*, 3, 36–41.
- 1171 Brunnacker, K., Löscher, M., Tillmans, W., Urban, B., 1982. Correlation of the Quaternary terrace  
1172 sequence in the lower Rhine valley and northern Alpine foothills of central Europe. *Quaternary*  
1173 *Research* 18, 152–173.
- 1174 Burkhalter, L., 1933. Note sur les stations préhistoriques du Gouvernement de Lattaquié. *Bulletin*  
1175 *de la Société Préhistorique Française* 30, 582–558.
- 1176 Butler, R.W.H., Spencer, S., 1999. Landscape evolution and the preservation of tectonic landforms  
1177 along the northern Yammouneh Fault, Lebanon. In: Smith, B.J., Whalley, W.B., Warke, P.A. (eds.),  
1178 *Uplift, Erosion, and Stability: Perspectives on Long-term Landscape Development*. Geological  
1179 *Society of London Special Publication* 162, 143–156.
- 1180 Çalışkan, V., 2008. Human-Induced Wetland Degradation: A case study of Lake Amik (Southern  
1181 Turkey). *Balwois (Ohrid, Republic of Macedonia)* 27, 1–10.
- 1182 Clark, J.D., 1966a. The Middle Acheulian occupation site at Latamne, northern Syria. *Annales*  
1183 *Archéologiques Arabes Syriennes* 16, 31–74.
- 1184 Clark, J.D., 1966b. Further excavations (1965) at the Middle Acheulian occupation site at Latamne,  
1185 northern Syria: general results, definitions and interpretations. *Annales Archéologiques Arabes*  
1186 *Syriennes* 16, 75–113.
- 1187 Clark, J.D., 1966c. Acheulian occupation sites in the Middle East and Africa: A study in cultural  
1188 variability. *American Anthropologist* 68, 202–229.
- 1189 Clark, J.D., 1967. The Middle Acheulian occupation site at Latamne, northern Syria. *Quaternaria* 9,  
1190 1–68.
- 1191 Clark, J.D., 1968. The Middle Acheulian occupation site at Latamne, northern Syria: Further  
1192 excavation. *Quaternaria* 10, 1–76
- 1193 Copeland, L., Hours, F., 1993. The Middle Orontes paleolithic flint industries. In: Sanlaville, P.,  
1194 Besançon, J., Copeland, L., Muhesen, S. (eds.), *Le Paléolithique de la vallée moyenne de l’Oronte*  
1195 *(Syrie): Peuplement et environnement*. *British Archaeological Review, International Series*, 587,  
1196 pp. 63–144.

- 1197 Dashora, A., Lohani, B., Malik, J.N., 2007. A repository of Earth resource information - CORONA  
1198 satellite programme. *Current Science* 92, 926–932.
- 1199 de Heinzelin, J., 1966. Geological observations near Latamne. *Annales Archeologiques Arabes*  
1200 *Syriennes*, 16, 115–120.
- 1201 de Heinzelin, J., 1968. Geological observations near Latamne. *Quaternaria* 10, 3–8.
- 1202 Demir, T., Yeşilnacar, İ., Westaway, R., 2004. River terrace sequences in Turkey: sources of  
1203 evidence for lateral variations in regional uplift. *Proceedings of the Geologists' Association* 115,  
1204 289–311.
- 1205 Demir, T., Seyrek, A., Guillou, H., Scaillet, S., Westaway, R., Bridgland, D., 2009. Preservation by  
1206 basalt of a staircase of latest Pliocene terraces of the River Murat in eastern Turkey: evidence for  
1207 rapid uplift of the eastern Anatolian Plateau. *Global and Planetary Change* 68, 254–269.
- 1208 Demir, T., Seyrek, A., Westaway, R., Bridgland, D., Beck, A., 2008. Late Cenozoic surface uplift  
1209 revealed by incision by the River Euphrates at Birecik, southeast Turkey. *Quaternary International*  
1210 186, 132–163.
- 1211 Demir, T., Westaway, R., Bridgland, D., Pringle, M., Yurtmen, S., Beck, A., Rowbotham, G., 2007.  
1212 Ar-Ar dating of Late Cenozoic basaltic volcanism in northern Syria: implications for the history of  
1213 incision by the River Euphrates and uplift of the northern Arabian Platform. *Tectonics* 26, doi:  
1214 10.1029/2006TC001959.
- 1215 Demir, T., Seyrek, A., Westaway, R., Guillou, H., Scaillet, S., Beck, A., Bridgland, D.R., this issue.  
1216 Late Cenozoic regional uplift and localised crustal deformation within the northern Arabian  
1217 Platform in southeast Turkey: investigation of the Euphrates terrace staircase using  
1218 multidisciplinary techniques. *Geomorphology*, this issue.
- 1219 Devyatkin, E.V., Dodonov, A.E., Sharkov, E.V., Zykin, V.S., Simakova, A.N., Khatib, K., Nseir,  
1220 H., 1997. The El-Ghab rift depression in Syria: its structure, stratigraphy and history of  
1221 development. *Stratigraphy and Geological Correlation* 5, 362–374.
- 1222 Dodonov, A.E., Deviatkin, E.V., Ranov, V.A., Khatib, K., Nseir, H., 1993. The Latamne Formation  
1223 in the Orontes river valley. In: Sanlaville, P., Besançon, J., Copeland, L., Muhesen, S. (Eds.), *Le*  
1224 *Paléolithique de la vallée moyenne de l'Oronte (Syrie): Peuplement et environnement*. *British*  
1225 *Archaeological Reports, International Series*, vol. 587, pp. 189–194.

- 1226 Domas, J. 1994. The Late Cenozoic of the Al Ghab Rift, NW Syria. *Sbornik Geologických Ved,*  
1227 *Antropozoikum* 21, 57–73.
- 1228 Dubertret, L., Vautrin, H., 1938. Sur l'existence du Pontien lacustre en Syrie et sur sa signification  
1229 tectonique. *Comptes Rendus Hebdomadaires des Séances de l'Académie des Sciences de Paris* 206,  
1230 69–71.
- 1231 Erol, O. 1963. Asi Nehri deltasının jeomorfolojisi ve dördüncü zaman denizakarsu şekilleri (Die  
1232 Geomorphologie des Orontes-deltas und der anschliessenden pleistozänen Strand- und Fluss-  
1233 terrassen, Provinz Hatay, Türkei). *İstanbul Üniversitesi Dil ve Tarih-Coğrafya Fakültesi Yayınları*  
1234 [Publications of the Faculty of Language and History-Geography of İstanbul University] 148, 1–  
1235 110 [in Turkish and German].
- 1236 Gábris, G., Nádor, A., 2007. Long-term fluvial archives in Hungary: response of the Danube and  
1237 Tisza rivers to tectonic movements and climatic changes during the Quaternary: a review and new  
1238 synthesis. *Quaternary Science Reviews* 26, 2758–2782.
- 1239 Galiatsatos, N., 2004. Assessment of the CORONA series of satellite imagery for landscape  
1240 archaeology: a case study from Orontes valley, Syria, PhD thesis, Durham University, United  
1241 Kingdom.
- 1242 Galiatsatos, N., Donoghue, D.N.M., Philip, G., 2008. High resolution elevation data derived from  
1243 stereoscopic CORONA imagery with minimal ground control: an approach using IKONOS and  
1244 SRTM data, *Photogrammetric Engineering & Remote Sensing* 74, 1093–1106.
- 1245 Galiatsatos, N., 2009. The shift from film to digital product: focus on CORONA imagery,  
1246 *Photogrammetrie - Fernerkundung - Geoinformation* 3, 251–260.
- 1247 Galiatsatos, N., Wilkinson, T.J., Donoghue, D.N.M., Philip, G., 2009. The Fragile Crescent Project  
1248 (FCP): Analysis of Settlement Landscapes Using Satellite Imagery. *CAA 2009: Making history*  
1249 *interactive*, Williamsburg, Virginia, USA.
- 1250 Gomez, F., Khawlie, M., Tabet, C., Darkal, A.N., Khair, K., Barazangi, M., 2006. Late Cenozoic  
1251 uplift along the northern Dead Sea transform in Syria and Lebanon. *Earth and Planetary Science*  
1252 *Letters* 241, 913–931.

- 1253 Gonçalves, J., and J.C. Fernandes, 2005. Assessment of SRTM-3 DEM in Portugal with  
1254 topographic map data, *Proceedings of the EARSeL Workshop 3D-Remote Sensing*, 10-11 June,  
1255 Porto, Portugal (European Association of Remote Sensing Laboratories), unpaginated CD-ROM.
- 1256 Goren-Inbar, N., Belitzky, S., 1989. Structural position of the Pleistocene Gesher Benot-Ya'aqov  
1257 site in the Dead Sea Rift Zone. *Quaternary Research* 31, 371–376.
- 1258
- 1259 Goren-Inbar, N., Belitzky, S., Verosub, K., Werker, E., Kislev, M., Heimann, A., Cari, I.,  
1260 Rosenfeld, A., 1992. New discoveries at the Middle Pleistocene Acheulian site of Gesher Benot  
1261 Ya'aqov, Israel. *Quaternary Research* 38, 117–128.
- 1262
- 1263 Goren-Inbar, N., Feibel, C.S., Verosub, K.L., Melamed, Y., Kislev, M.E., Tchernov, E., Saragusti,  
1264 I., 2000. Pleistocene milestones on the out-of-Africa corridor at Gesher Benot Ya'aqov, Israel.  
1265 *Science* 289, 944–948
- 1266 Guérin, C., Faure, M., 1988 Biostratigraphie comparée des grands mammifères du Pléistocène en  
1267 Europe Occidentales et au Moyen Orient. *Paléorient* 14/2, 50–56
- 1268 Guérin, C., Eisenmann, V., Faure, M., 1993. Les grands mammifères du gisement Pléistocène  
1269 Moyen de Latamné (vallée de l'Oronte, Syrie). In: Sanlaville, P., Besançon, J., Copeland, L.,  
1270 Muhesen, S. (eds.), *Le Paléolithique de la vallée moyenne de l'Oronte (Syrie): Peuplement et*  
1271 *environnement*. *British Archaeological Review, International Series*, 587, pp. 169–178.
- 1272 Heimann, A., Steinitz, G., 1989.  $^{40}\text{Ar}/^{39}\text{Ar}$  total gas ages of basalts from Notera 3 well, Hula Valley,  
1273 Dead Sea Rift: stratigraphic and tectonic implications. *Israel Journal of Earth Science* 38, 173–184.
- 1274 Heimann, A., Zilberman, E., Amit, R., Frieslander, U., 2009. Northward migration of the southern  
1275 diagonal fault of the Hula pull-apart basin, Dead Sea Transform, northern Israel. *Tectonophysics*  
1276 476, 496–511.
- 1277 Heller, J., 2007. A historic biogeography of the aquatic fauna of the Levant. *Biological Journal of*  
1278 *the Linnean Society* 92, 625–639.
- 1279
- 1280 Holmes, J.A., 1996. Trace-element and stable-isotope geochemistry of non-marine ostracod shells  
1281 in Quaternary palaeoenvironmental reconstruction. *Journal of Paleolimnology* 15, 223–235.
- 1282 Hooijer, D.A., 1961. Middle Pleistocene mammals from Latamne, Orontes Valley, Syria. *Annales*  
1283 *Archéologiques de Syrie*, 11, 117–132.

1284  
1285 Hooijer, D.A., 1965. Additional notes on the Pleistocene mammalian fauna of the Orontes valley.  
1286 *Annales Archéologiques de Syrie* 15, 101–104.  
1287  
1288 Ivanovich, M., Latham, A.G., Ku, T.L., 1992. Uranium-series disequilibrium applications in  
1289 geochronology. In: *Uranium-series disequilibrium: applications to Earth, marine and environmental*  
1290 *science, Second Edition* (Ivanovich, M., Harmon, R.S. Eds.). Oxford University Press, Oxford, 62–  
1291 94.  
1292  
1293 Jacobsen, K., 2005. Analyses of SRTM elevation models, *Proceedings of the EARSeL Workshop*  
1294 *3D-Remote Sensing, 10-11 June, Porto, Portugal* (European Association of Remote Sensing  
1295 Laboratories), unpaginated CD-ROM.  
  
1296 JPL (Jet Propulsion Laboratory) 1998a. Shuttle Radar Topographic Mission: mapping the world in  
1297 three dimensions. Jet Propulsion Laboratory, California Institute of Technology, Pasadena,  
1298 California. JPL report 400-713 7/98. Available online:  
1299 [http://www2.jpl.nasa.gov/srtm/factsheet\\_tech.pdf](http://www2.jpl.nasa.gov/srtm/factsheet_tech.pdf)  
  
1300 JPL 1998b. Seeing Earth's surface in 3-D: Shuttle Radar Topographic Mission. Jet Propulsion  
1301 Laboratory, California Institute of Technology, Pasadena, California. JPL report 400-714 7/98.  
1302 Available online: [http://www2.jpl.nasa.gov/srtm/factsheet\\_pub.pdf](http://www2.jpl.nasa.gov/srtm/factsheet_pub.pdf)  
  
1303 JPL 2005. Shuttle Radar Topographic Mission: the mission to map the world. Jet Propulsion  
1304 Laboratory, California Institute of Technology, Pasadena, California. Available online:  
1305 <http://www2.jpl.nasa.gov/srtm/index.html>  
  
1306 Kafri, U., Kaufman, A., Magaritz, M., 1983. The rate of Pleistocene subsidence and sedimentation  
1307 in the Hula Basin as compared with those of other time spans in other Israeli tectonic regions. *Earth*  
1308 *and Planetary Science Letters* 65, 126–132.  
  
1309 Kasse, C., Bohncke, S.J.P., Vandenberghe, J., Gábris, G. 2010. Fluvial style changes during the last  
1310 glacial–interglacial transition in the middle Tisza valley (Hungary). *Proceedings of the Geologists'*  
1311 *Association* 121, 180–194.  
  
1312 Kay, S., P. Spruyt., R. Zielinski, P. Winkler, S. Mihály, and G. Ivan, 2005. Quality checking of  
1313 DEM derived from satellite data (SPOT and SRTM), *Proceedings of the EARSeL Workshop 3D-*

- 1314 *Remote Sensing*, 10-11 June, Porto, Portugal (European Association of Remote Sensing  
1315 Laboratories), unpaginated CD-ROM.
- 1316 Kelley, S.P., 2002. K–Ar and Ar–Ar dating. *Reviews in Mineralogy and Geochemistry* 47, 785–  
1317 818.
- 1318 Kiliç, S., Evrendilek, F., Berberoğlu, B., Demirkesen, A.C., 2006. Environmental monitoring of  
1319 land-use and land-cover changes in Amik Plain, Turkey. *Environmental Monitoring and*  
1320 *Assessment* 114, 157–168.
- 1321 Koenigswald, W. von, Fejfar, O., Tchernov, E. 1992. Revision einiger alt- und mittelpleistozaner  
1322 arvicoliden (Rodentia, Mammalia) aus dem östlichen Mittelmeergebiet ('Ubeidiya, Jerusalem und  
1323 Kalymnos–Xi). *Neues Jahrbuch für Geologie und Paläontologie, Abhandlungen* 184, 1–23.
- 1324 Lister, A.M., Sher, A.V., 2001. The origin and evolution of the woolly mammoth. *Science*, 294,  
1325 1094–1097.
- 1326 McLaren, S., 2004. Characteristics, evolution and distribution of Quaternary channel calcretes,  
1327 southern Jordan. *Earth Surface Processes and Landforms* 29, 1487–1507.
- 1328 Markova, A., 2007. Pleistocene chronostratigraphic subdivisions and stratigraphic boundaries in the  
1329 mammal record. *Quaternary International* 160, 100–111.
- 1330 Mein, P., Besançon, J., 1993. Micromammifères du Pléistocène Moyen de Letamn . In: Sanlaville,  
1331 P., Besançon, J., Copeland, L., Muhesen, S. (eds.), *Le Pal olithique de la vall e moyenne de*  
1332 *l'Oronte (Syrie): Peuplement et environnement*. *British Archaeological Review, International*  
1333 *Series*, 587, pp 179–182.
- 1334 Meyer, W., Stets, J., 2002. Pleistocene to Recent tectonics in the Rhenish Massif (Germany).  
1335 *Netherlands Journal of Geosciences / Geologie en Mijnbouw* 81, 217–221.
- 1336 Modderman, P.J.R., 1964. On a survey of Palaeolithic sites near Hama. *Annales Arch ologiques*  
1337 *Arabes Syriennes* 14, 51–66.
- 1338 Moshkovitz, S., Magaritz, M., 1987. Stratigraphy and isotope records of Middle and Late  
1339 Pleistocene mollusks from a continuous corehole in the Hula Basin, Northern Jordan Valley, Israel.  
1340 *Quaternary Research* 28, 226–237.
- 1341

- 1342 Mouty, M., Delaloye, M., Fontignie, D., Piskin, O., Wagner, J.-J., 1992. The volcanic activity in  
1343 Syria and Lebanon between Jurassic and Actual. *Schweiz. Mineral. Petrogr. Mitt.*, 72, 91–105.
- 1344 Muhsen, S. 1985. *L'Acheuléen Récent Évolué de Syrie*. British Archaeological Reports,  
1345 International Series 248, Archaeopress, Oxford.
- 1346 Nash, D.J., Smith, R.F., 1998. Multiple calcrete profiles in the Tabernas Basin, southeast Spain:  
1347 their origins and geomorphic implications. *Earth Surface Processes and Landforms* 23, 1009–1029.
- 1348 Nash, D.J., Smith, R.F., 2003. Properties and development of channel calcretes in a mountain  
1349 catchment, Tabernas Basin, southeast Spain. *Geomorphology* 50, 227–250.
- 1350 Perinçek, D., Çemen, İ., 1990. The structural relationship between the East Anatolian and Dead Sea  
1351 fault zones in southeastern Turkey. *Tectonophysics* 172, 331–340.
- 1352 Philip, G., Abdulkarim, M., Newson, P., Beck, A., Bridgland, D., Bshesh, M., Shaw, A., Westaway,  
1353 R., Wilkinson, K. 2005. Settlement and landscape development in the Homs Region, Syria : report  
1354 on work undertaken during 2001–2003. *Levant* 37, 21–42.
- 1355 Picard, L., 1963. The Quaternary in Northern Jordan Valley. *Proceedings of Israel Academy of*  
1356 *Science and Humanities* 1, 1–34.
- 1357
- 1358 Pirazzoli, P.A., Laborel, J., Saliège, J.F., Erol, O., Kayan, İ, Person, A., 1991. Holocene raised  
1359 shorelines on the Hatay coasts (Turkey): palaeoecological and tectonic implications. *Marine*  
1360 *Geology* 96, 295–311.
- 1361 Ponikarov, V. (Ed.), 1986. *Geological Map of Syria (1: 1,000,000; 2nd Edition)*. Establishment of  
1362 *Geology and Mineral Resources (Ministry of Petroleum and Mineral Resources)*, Syrian Arab  
1363 Republic.
- 1364 Ponikarov, V., Kozlov, V., Artemov, A., Kalis, A., 1963a. Geological map of Syria, 1:200,000  
1365 scale, sheet I-36-XVIII, I-37-XIII, Homs-Trablus. Technoexport, Moscow, and Ministry of  
1366 Industry, Damascus.
- 1367 Ponikarov, V., Shatsky, V., Kazmin, V., Mikhailov, I., Aistov, L., Kulakov, V., Shatskaya, M.,  
1368 Shirokov, V., 1963b. Geological map of Syria, 1:200,000 scale, sheet I-36-XXIV, I-37-XIX, Hama-  
1369 Latheqieh. Technoexport, Moscow, and Ministry of Industry, Damascus.

- 1370 Rodriguez, E., Morris, C.S., Belz, J.E., 2006. A global assessment of the SRTM performance.  
1371 Photogrammetric Engineering & Remote Sensing 72, 249–260.
- 1372 Ruegg, G.H.J., 1994. Alluvial architecture of the Quaternary Rhine–Meuse river system in the  
1373 Netherlands. *Geologie en Mijnbouw* 72, 321–330.
- 1374 Sanlaville, P., 1988. Synthèse sur le paléoenvironnement. *Paléorient* 14, 57–60.
- 1375 Schattner, U., Weinberger, R., 2008. A mid-Pleistocene deformation transition in the Hula Basin,  
1376 northern Israel: implications for the tectonic evolution of the Dead Sea Fault. *Geochemistry,  
1377 Geophysics, Geosystems* 9, Q07009, doi: 10.1029/2007GC001937, 18 pp.
- 1378
- 1379 Schütt, H., 1988. Ergänzungen zur Kenntnis der Molluskenfauna oberpliozäner Süßwasser  
1380 konglomerate Syriens. *Archiv für Molluskenkunde* 118, 129–143.
- 1381
- 1382 Searle, M.P., Chung Sun-Lin, Lo Ching-Hua, 2010. Geological offsets and age constraints along the  
1383 northern Dead Sea fault, Syria. *Journal of the Geological Society, London* 167, 1001–1008.
- 1384
- 1385 Seyrek, A., Demir, T., Pringle, M., Yurtmen, S., Westaway, R., Bridgland, D., Beck, A.,  
1386 Rowbotham, G., 2008. Late Cenozoic uplift of the Amanos Mountains and incision of the Middle  
1387 Ceyhan river gorge, southern Turkey; Ar–Ar dating of the Düzici basalt. *Geomorphology* 97, 321–  
1388 355.
- 1389
- 1390 Seyrek, A., Demir, T., Pringle, M., Yurtmen, S., Westaway, R., Beck, A., Rowbotham, G., 2007.  
1391 Kinematics of the Amanos Fault, southern Turkey, from Ar–Ar dating of offset Pleistocene basalt  
1392 flows: transpression between the African and Arabian plates. In: Cunningham, W.D., Mann, P.  
1393 (Eds.), *Tectonics of Strike-slip Restraining and Releasing Bends*. Geological Society, London,  
1394 Special Publication 290, 255–284.
- 1395
- 1396 Sharkov, E.V., Chernyshev, I.V., Devyatkin, E.V., Dodonov, A.E., Ivanenko, V.V., Karpenko, M.I.,  
1397 Leonov, Y.G., Novikov, V.M., Hanna, S., Khatib, K., 1994. Geochronology of Late Cenozoic  
1398 basalts in western Syria. *Petrology*, 2 (4), 385–394 [Russian original: *Petrologiya*, 2 (4), 439–448].
- 1399
- 1400 Sharkov, E.V., Chernyshev, I.V., Devyatkin, E.V., Dodonov, A.E., Ivanenko, V.V., Karpenko, M.I.,  
1401 Lebedev, V.A., Novikov, V.M., Hanna, S., Khatib, K., 1998. Novye dannye po geochronologii  
1402 Pozdnekainozoiskich platobazaltov severo-vostochnoi periferii Krasnomorskoi riftovoi oblasti

1403 (severnaya Siriya) [New data on the geochronology of the Late Cenozoic plateau basalt of the  
1404 northeast margin of the Red Sea rift region (northern Syria)]. *Doklady Akademii Nauk* 358, 96–99.  
1405  
1406 Shaw, A.D., 2008. *The Earlier Palaeolithic of Syria: Settlement History, Technology and*  
1407 *Landscape-use in the Orontes and Euphrates Valleys*. Unpublished Ph.D Thesis, University of  
1408 Durham.  
1409  
1410 Shaw, A.D. (in press). *The Earlier Palaeolithic of Syria: Reinvestigating the Orontes and Euphrates*  
1411 *Valleys*. Southampton Monographs in Archaeology. Archaeopress, Oxford.  
1412  
1413 Sivan, N., Heller, J., Van Damme, D., 2006. Fossil Viviparidae (Mollusca: Gastropoda) of the  
1414 Levant. *Journal of Conchology* 39, 207–219.  
1415  
1416 Sohn, H.G., Kim, G., Yom, J., 2004. Mathematical modelling of historical reconnaissance  
1417 CORONA KH-4B imagery. *The photogrammetric record* 19, 51–66.  
1418  
1419 Tchernov, E., 1973. On the Pleistocene Molluscs of the Jordan Valley. *Israel Academy of Science*  
1420 *and Humanities*, Jerusalem.  
1421  
1422 Tchernov, E., 1987. The age of the ‘Ubeidiya Formation, an Early Pleistocene hominid site in the  
1423 Jordan Valley, Israel. *Israel Journal of Earth Sciences* 36, 3–30.  
1424  
1425 Tchernov, E., 1999. The earliest hominids in the southern Levant. In: *Proceedings of the*  
1426 *International Conference of Human Palaeontology, Orce, Spain, 1995*. Museo de Prehistoria y  
1427 *Paleontologia, Orce, Spain*, pp. 389–406.  
1428  
1429 Tolun, N., Erentöz, C. 1962. Hatay sheet of the Geological Map of Turkey, 1:500,000 scale.  
1430 General Directorate of Mineral Research and Exploration, Ankara.  
1431  
1432 Ünay, E., Göktaş, F., Hakyemez, H.Y., Avşar, M., Şan, Ö., 1995. Büyük Menderes Grabeni’nin  
1433 kuzey kenarındaki çökellerin Arvicolidae (Rodentia, Mammalia) faunasma dayalı olarak  
1434 yaşlandırılması [Age determination of the sediments of the northern margin of the Büyük  
1435 Menderes graben based on their Arvicolidae (Rodentia, Mammalia) fauna]. *Geological Society of*  
1436 *Turkey Bulletin* 38, 75–80 (in Turkish with English abstract).  
1437

- 1438 Ünay, E., Emre, Ö., Erkal, T., Keçer, M., 2001. The rodent fauna from the Adapazarı pull-apart  
1439 basin (NW Anatolia): its bearings on the age of the North Anatolian fault. *Geodinamica Acta* 14,  
1440 169–175.
- 1441
- 1442 Van Liere, W.J., 1960. Un gisement Paléolithique dans un niveau Pleistocène de l'Oronte à Latamné  
1443 (Syrie). *Annales Archéologiques de Syrie* 10, 165–174.
- 1444 Van Liere, W.J., 1961. Observations on the Quaternary in Syria. *Berichten Rijksd. Ovdheidk.*  
1445 *Bodemonderzoek*, 11, 7–69.
- 1446 Van Liere, W.J., 1966. The Pleistocene and Stone Age of the Orontes. *Annales Archéologiques*  
1447 *Arabes Syriennes* 16, 7–30.
- 1448 Van Liere, W.J., Hooijer, D.A., 1961. A paleo-Orontes level with *Archidiskodon meridionalis*  
1449 (Nesti) at Hama. *Annales Archéologiques de Syrie*, 11, 165–172.
- 1450 Westaway, R., 2002. The Quaternary evolution of the Gulf of Corinth, central Greece: coupling  
1451 between surface processes and flow in the lower continental crust. *Tectonophysics* 348, 269–318.
- 1452 Westaway, R., 2004a. Pliocene and Quaternary surface uplift revealed by sediments of the Loire-  
1453 Allier river system, France. *Quaternaire* 15, 103–115.
- 1454 Westaway, R., 2004b. Kinematic consistency between the Dead Sea Fault Zone and the Neogene  
1455 and Quaternary left-lateral faulting in SE Turkey. *Tectonophysics* 391, 203–237.
- 1456 Westaway, R., 2006. Investigation of coupling between surface processes and induced flow in the  
1457 lower continental crust as a cause of intraplate seismicity. *Earth Surface Processes and Landforms*  
1458 31, 1480–1509.
- 1459 Westaway, R., 2010. The relationship between initial (end-Pliocene) hominin dispersal and  
1460 landscape evolution in the Levant; an alternative view. *Quaternary Science Reviews* 29, 1491–  
1461 1500.
- 1462 Westaway, R., 2011. Discussion of ‘Geological offsets and age constraints along the northern Dead  
1463 Sea fault, Syria’ by Michael P. Searle, Sun-Lin Chung, and Ching-Hua Lo (*Journal of the*  
1464 *Geological Society, London*, 167, 1001–1008, 2010). *Journal of the Geological Society, London*,  
1465 168, 621–623.

- 1466 Westaway, R., this issue. A numerical modelling technique that can account for alternations of  
1467 uplift and subsidence revealed by Late Cenozoic fluvial sequences. *Geomorphology*, this issue.
- 1468 Westaway, R., Bridgland, D.R., Mishra, S., 2003. Rheological differences between Archaean and  
1469 younger crust can determine rates of Quaternary vertical motions revealed by fluvial  
1470 geomorphology. *Terra Nova* 15, 287–298.
- 1471 Westaway, R., Bridgland, D.R., Sinha, R., Demir, T. 2009. Fluvial sequences as evidence for  
1472 landscape and climatic evolution in the Late Cenozoic: A synthesis of data from IGCP 518. *Global  
1473 & Planetary Change* 68, 237–253.
- 1474 Westaway, R., Maddy, D., Bridgland, D., 2002. Flow in the lower continental crust as a mechanism  
1475 for the Quaternary uplift of south-east England: constraints from the Thames terrace record.  
1476 *Quaternary Science Reviews* 21, 559–603.
- 1477 Westaway, R., Bridgland, D., White, M., 2006. The Quaternary uplift history of central southern  
1478 England: evidence from the terraces of the Solent River system and nearby raised beaches.  
1479 *Quaternary Science Reviews* 25, 2212–2250.
- 1480 Westaway, R., Demir, T., Seyrek, A., 2008. Geometry of the Turkey-Arabia and Africa-Arabia  
1481 plate boundaries in the latest Miocene to Mid-Pliocene: the role of the Malatya-Ovacık Fault Zone  
1482 in eastern Turkey. *eEarth* 3, 27–35.
- 1483 Westaway, R., Demir, T., Seyrek, A., Beck, A., 2006. Kinematics of active left-lateral faulting in  
1484 southeast Turkey from offset Pleistocene river gorges: improved constraint on the rate and history  
1485 of relative motion between the Turkish and Arabian plates. *Journal of the Geological Society,  
1486 London* 163, 149–164.
- 1487 Westaway, R., Guillou, H., A. Seyrek, T. Demir, D. Bridgland, S. Scaillet, A. Beck, 2009b. Late  
1488 Cenozoic surface uplift, basaltic volcanism, and incision by the River Tigris around Diyarbakır, SE  
1489 Turkey. *International Journal of Earth Sciences* 98, 601–625.
- 1490 Westaway, R., Bridgland, D.R., Sinha, R., Demir, T. 2009a. Fluvial sequences as evidence for  
1491 landscape and climatic evolution in the Late Cenozoic: a synthesis of data from IGCP 518. *Global  
1492 and Planetary Change* 68, 237–253.

- 1493 Wilkinson, T.J., 1997. The History of the Lake of Antioch: a preliminary note. In: Young, G.D.,  
1494 Chavalas, M.W., Averbeck, R.E. (Eds), *Crossing Boundaries and Linking Horizons: Studies in*  
1495 *Honor of Michael C. Astour on his 80th Birthday*. CDL Press, Bethesda, Maryland, pp. 557–576.
- 1496 Wright, V.P., Tucker, M.E., 1991. Calcretes: an introduction. In: *Calcrete* (Wright, V.P., Tucker,  
1497 M.E., Eds.). International Association of Sedimentologists Special Publication, No. 2, Blackwell  
1498 Scientific Publications, Oxford, pp. 1–22.
- 1499 Yener, K.A., Edens, C., Harrison, T.P., Verstraete, J., Wilkinson, T.J., 2000. The Amuq Valley  
1500 Regional Project. 1995–1998. *American Journal of Archaeology* 104, 163–220.
- 1501 Yurtmen, S., Guillou, H., Westaway, R., Rowbotham, G., Tatar, O., 2002. Rate of strike-slip  
1502 motion on the Amanos Fault (Karasu Valley, southern Turkey) constrained by K-Ar dating and  
1503 geochemical analysis of Quaternary basalts. *Tectonophysics* 344, 207–246.